Galerkin and Collocation Meshfree Methods: From Continuum to Quantum

J. S. Chen
Chancellor's Professor

Civil & Environmental Engineering Department
Mechanical & Aerospace Engineering Department
Mathematics Department
University of California, Los Angeles (UCLA)
Los Angeles, CA 90095, USA

http://www.cee.ucla.edu/faculty/jschen.htm

UCLA

UCLA 特色

- **1919**年成立，目前教職員及學生超過**4**萬人
- 世界前五百大學中排名十三
- 美國新聞暨世界調查報告－全美排名第二至四公立大學
- 過去**10**年有**2**位諾貝爾獎得主，總共**5**位諾貝爾獎得主， 曾有**4**位諾貝爾獎得主是從**UCLA**畢業
- **2006** 年費爾茲獎得主－ **UCLA**數學系 陶哲軒 教授
- **59**位國家院士（**31**科學院院士、**22**工程院院士、**6**教育院院士），**90**位美國藝術及科學院院士，**30**位醫學院院士，**3**項國家科學獎

UCLA

UCLA Henry Samueli School of Engineering and Applied Science

- 全美研究單位平均指導博士生排名第一
- 全美研究單位平均研究經費排名第六
- 該院**14**%的教師榮獲全美工程院或科學院會士榮銜
- 網際網路及無線網路技術的發源地
- 共**21**個主要研究中心，**7**個研究中心於近**4**年成立
  - **California NanoSystems Institute**
  - **Center for Embedded Networked Sensing**
  - **Institute for Cell Mimetic Space Exploration**
  - **Western Institute of Nanoelectronics**
  - **Functional Engineered Nano Architectonics Focus Center**
  - **Center for Cell Control**
  - **Center for Scalable and Integrated Nano-Manufacturing**

Civil & Environmental Engineering Department

Environmental Engineering

- **E. M. V. Hoek** Nanotechnology, membranes, colloidal chemistry, water treatment, desalination
- **J. A. Jay** Aquatic chemistry, environmental microbiology.
- **M. K. Stenstrom** Process development and control for water and wastewater treatment plants
- **K. D. Stolzenbach** Environmental fluid mechanics and transport.

E. M. V. Hoek

J. A. Jay

M. K. Stenstrom

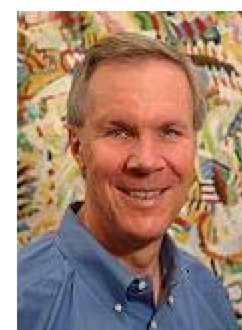

K. D. Stolzenbach

UCLA

Civil & Environmental Engineering Department

Geotechnical Engineering

- **S. J. Brandenberg** Geotechnical earthquake engineering with a focus on soil-structure interaction, liquefaction, data acquisition and processing, and numerical analysis.
- **J. P. Stewart** Earthquake Geotechnical Engineering with emphasis on soil-structure interaction, site effects on ground motion, and ground failure
- **M. Vucetic** Geotechnical engineering, soil dynamics, geotechnical earthquake engineering, laboratory testing of soils

S. J. Brandenberg

J. P. Stewart

M. Vucetic

UCLA

Civil & Environmental Engineering Department

Structural Engineering & Mechanics

- **J. S. Chen** Computational mechanics (finite element method and meshless method); solid mechanics; materials modeling; biomechanics; quantum mechanics.
- **J. W. Ju** Damage mechanics, micromechanics of composites, computational mechanics, nanomechanics, NDE, fracture mechanics, and biomechanics.
- **E. Taciroglu** Computational solid and structural mechanics, earthquake engineering
- **J. W. Wallace** Earthquake engineering, design methodologies, seismic evaluation and retrofit, large-scale testing laboratory and field studies/testing.
- **J. Zhang** Earthquake engineering, structural dynamics and mechanics, seismic protective devices and strategies, soil-structure interaction and bridge engineering.

J. S. Chen | J. W. Ju | E. Taciroglu | J. W. Wallace | J. Zhang

UCLA

Civil & Environmental Engineering Department

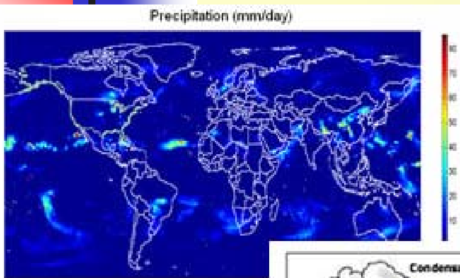

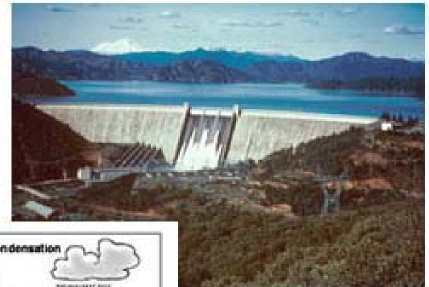

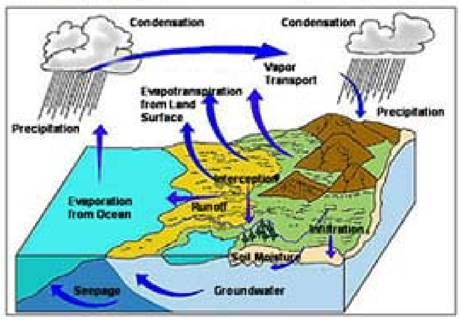

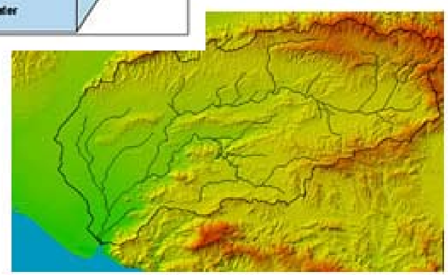

Hydrology and Water Resources Engineering

•**T. S. Hogue** Surface hydrology, rainfall-runoff and land-surface modeling, operational flood forecasting, optimization techniques.

•**S. A. Margulis** Surface hydrology, hydrometeorology, remote sensing, and data assimilation.

•**W. W-G. Yeh** Groundwater hydrology, modeling of solute transport in groundwater, optimization of water resources systems.

T. S. Hogue

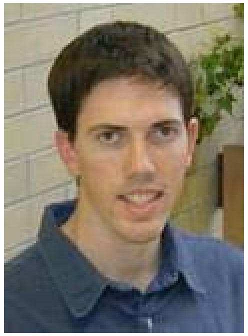

S. A. Margulis

W. W-G. Yeh

UCLA

Galerkin and Collocation Meshfree Methods: From Continuum to Quantum

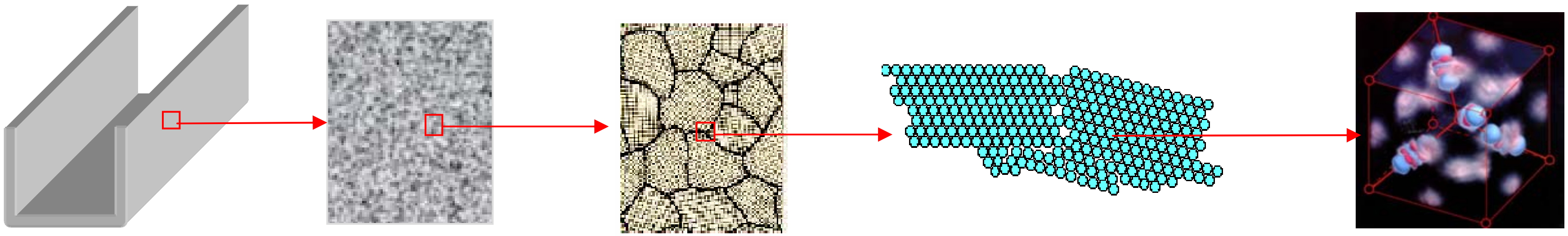

Are We Solving the Right Equations?
Are We Solving the Equations Right?

Challenges in Multiscale Computation:

- Regularity requirement: smoothness, roughness
- Multiple length scales, scale coupling
- Multiple physics, interactions
- Geometry complexity, topological changes

UCLA

Numerical Solution of PDEs

Approximation

- Local Polynomials
- Moving Least Squares/ Reproducing Kernel
- Laplace Interpolant
- Radial Basis Functions
- Splines /Rational B-Splines
- Smooth Kernel
- Local Polynomials with Enrichment
- MLS/RK with Enrichment

Discretization

- Galerkin Weak Form
  - Gauss Integration
  - Point Collocation
  - Nodal Integration w. Stabilization
- Petrov Galerkin
  - Gauss Integration
- Strong Form
  - Point Collocation
  - Subdomain Collocation
- Lagrangian-Euler Form

Methods

- FEM
- SPH
- C-SPH
- EFG/RKPM
- S-EFG/RKPM
- PUFEM/GFEM
- HP- Clouds
- XFEM
- MLPG
- NEM
- S-NEM
- MPM
- RBCM

UCLA

Outline

- **Galerkin Meshfree Method**
  - MLS/RK Approximation
  - Spatial & Temporal Stability
  - Semi-Lagrangian Discretization
  - Applications

- **Radial Basis Collocation Method**
  - Weighted RBCM
  - Localized RBF

Moving Least Squares/Reproducing Kernel Approximation

(Liu, 1995, Chen 1996)

Correction function

$$C(\boldsymbol{x};\boldsymbol{x}-\boldsymbol{x}_I)$$
$$=\sum_{i+j+k=0}^{n}(x_1-x_{1I})^i(x_2-x_{2I})^j(x_3-x_{3I})^k\, b_{ijk}(\boldsymbol{x})$$

Completeness

Consistency

$$u^h(\boldsymbol{x})=\sum_{I=1}^{NP}\overbrace{C(\boldsymbol{x};\boldsymbol{x}-\boldsymbol{x}_I)}\underbrace{\Phi_a(\boldsymbol{x}-\boldsymbol{x}_I)}d_I\equiv\sum_{I=1}^{NP}\Psi_I(\boldsymbol{x})d_I$$

Kernel function $\Phi_a(\boldsymbol{x}-\boldsymbol{x}_I)$

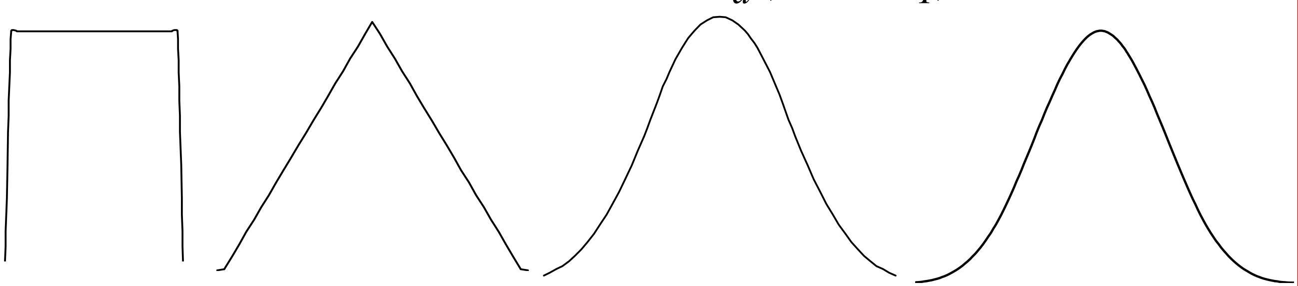

Box Function **Hat Function** **Quadratic B-spline** **Cubic B-spline**

Smoothness

Locality

Discrete Reproducing Kernel Approximation

Reproducing Conditions

$$\sum_{I=1}^{NP} \Psi_I(\boldsymbol{x}) x_{1I}^i x_{2I}^j x_{3I}^k = x_1^i x_2^j x_3^k \ , i+j+k = 0, \cdots, n$$

$$\Longrightarrow \boldsymbol{b}(\boldsymbol{x}; \boldsymbol{x}-\boldsymbol{x}_I) = \boldsymbol{M}^{-1}(\boldsymbol{x}) \boldsymbol{H}(\boldsymbol{x}-\boldsymbol{x}_I)$$

$$\boldsymbol{M}(\boldsymbol{x}) = \sum_{I=1}^{NP} \boldsymbol{H}(\boldsymbol{x}-\boldsymbol{x}_I) \boldsymbol{H}^T(\boldsymbol{x}-\boldsymbol{x}_I) \Phi_a(\boldsymbol{x}-\boldsymbol{x}_I)$$

$$\boldsymbol{H}^T(\boldsymbol{x}-\boldsymbol{x}_I) = [1, x_1 - x_{1I}, \cdots, (x_3 - x_{3I})^n]$$

Reproducing Kernel Approximation

$$u^h(\boldsymbol{x}) = \sum_{I=1}^{NP} \Psi_I(\boldsymbol{x}) d_I$$

$$\Psi_I(\boldsymbol{x}) = \boldsymbol{H}^T(\boldsymbol{0}) \boldsymbol{M}^{-1}(\boldsymbol{x}) \boldsymbol{H}(\boldsymbol{x}-\boldsymbol{x}_I) \Phi_a(\boldsymbol{x}-\boldsymbol{x}_I)$$

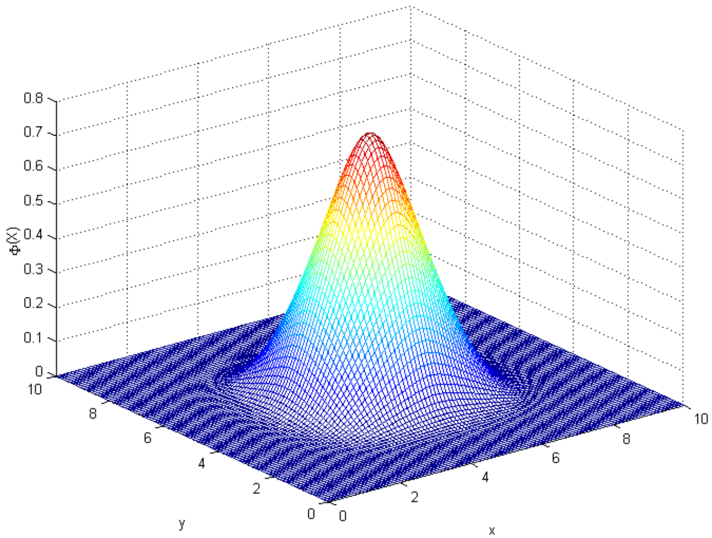

Meshfree Shape Function

UCLA

Domain Discretization

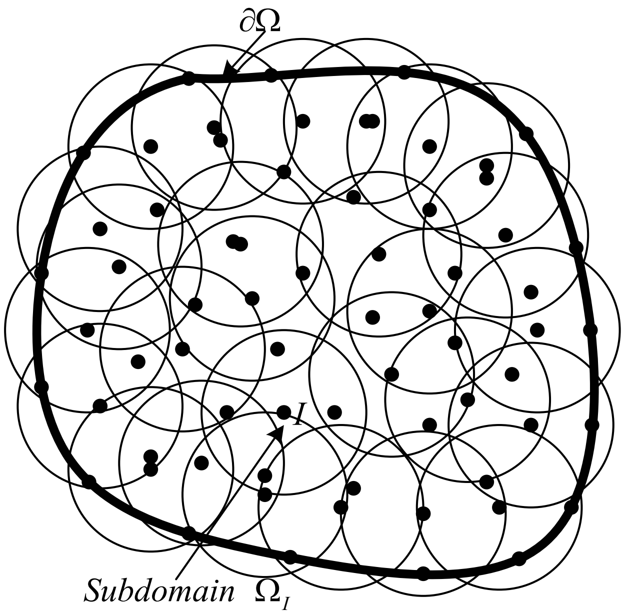

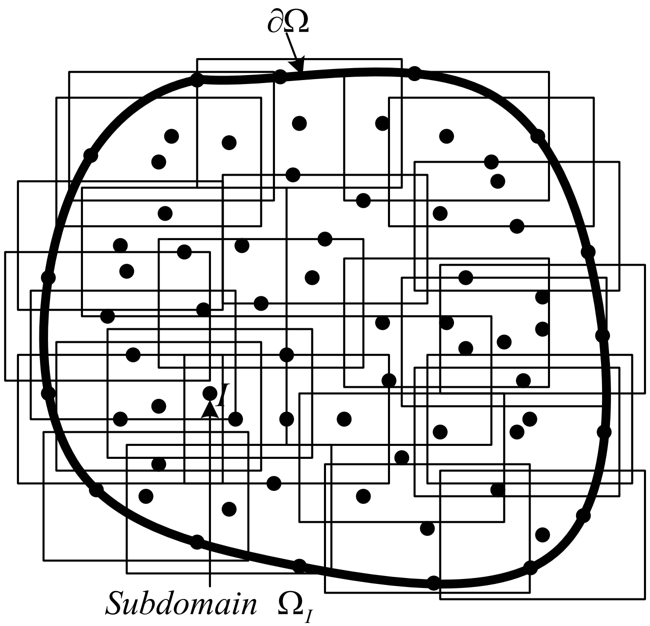

Domain Discretization

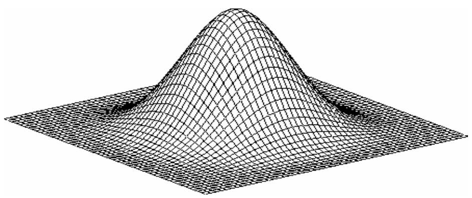

Shape Function

Galerkin Approximation

Strong Form of linear elasticity

$$\left(C_{ijkl}u_{(k,l)}\right),_j + b_i = 0 \quad in \quad \Omega$$

$$u_i = g_i \quad on \quad \Gamma^g$$

$$\left(C_{ijkl}u_{(k,l)}\right)n_j = h_i \quad on \quad \Gamma^h$$

Weak Form

$$\int_\Omega \delta u_{(i,j)} C_{ijkl} u_{(k,l)} d\Omega + \int_{\Gamma^g} \delta\lambda_i (u_i - g_i) d\Gamma + \int_{\Gamma^g} \delta u_i \lambda_i d\Gamma = \int_\Omega \delta u_i b_i d\Omega + \int_{\Gamma^h} \delta u_i h_i d\Gamma$$

$$\forall u_i \in H^1, \lambda_i \in H^0$$

Galerkin Approximation

$$u_i^h = \sum \Psi_I d_{iI} \quad , \quad \lambda_i^h = \sum N_I \lambda_{iI}$$

$$\Rightarrow \begin{bmatrix} \boldsymbol{K} & \boldsymbol{G} \\ \boldsymbol{G}^T & \boldsymbol{0} \end{bmatrix} \begin{bmatrix} \boldsymbol{d} \\ \boldsymbol{\lambda} \end{bmatrix} = \begin{bmatrix} \boldsymbol{f} \\ \boldsymbol{q} \end{bmatrix}, \qquad \boldsymbol{K}_{IJ} = \int_\Omega \boldsymbol{B}_I^T \boldsymbol{C} \boldsymbol{B}_J d\Omega, \qquad \boldsymbol{f}_I = \int_\Omega \Psi_I \boldsymbol{b} d\Omega + \int_{\Gamma^h} \Psi_I \boldsymbol{h} d\Gamma$$

UCLA

Convergence Properties of Meshfree Methods
Effect of Basis Functions (Poisson Problem)

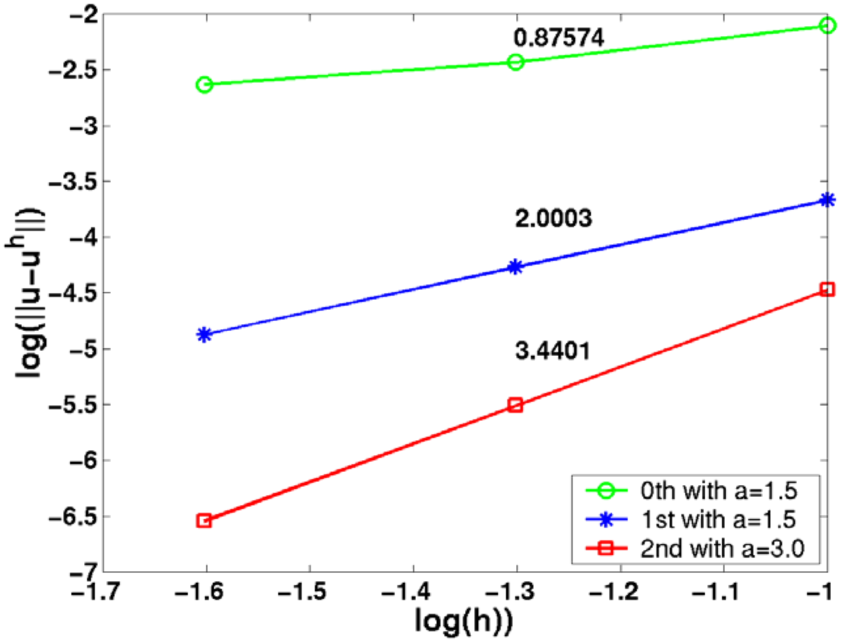

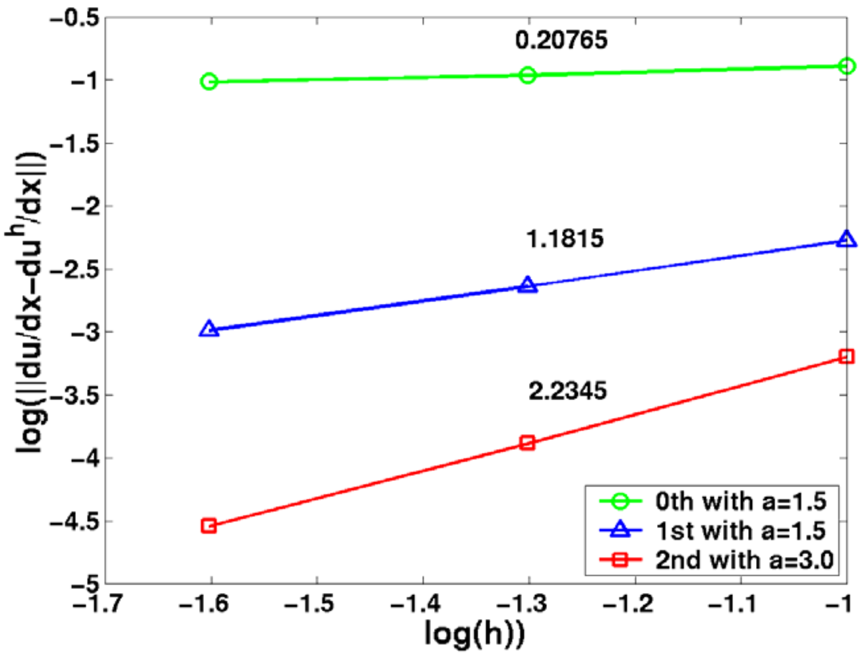

UCLA

Convergence Properties of Meshfree Methods
Effect of Support Size

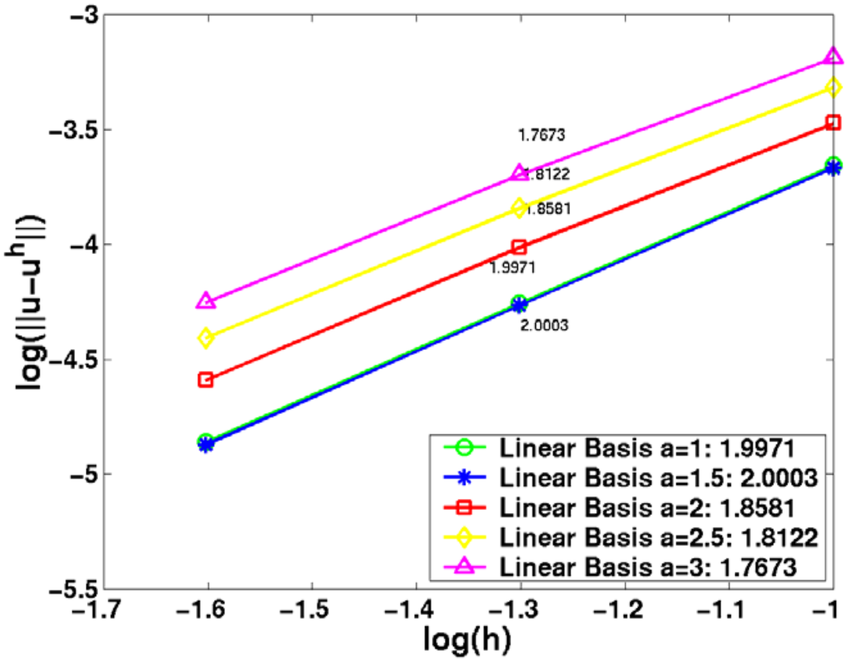

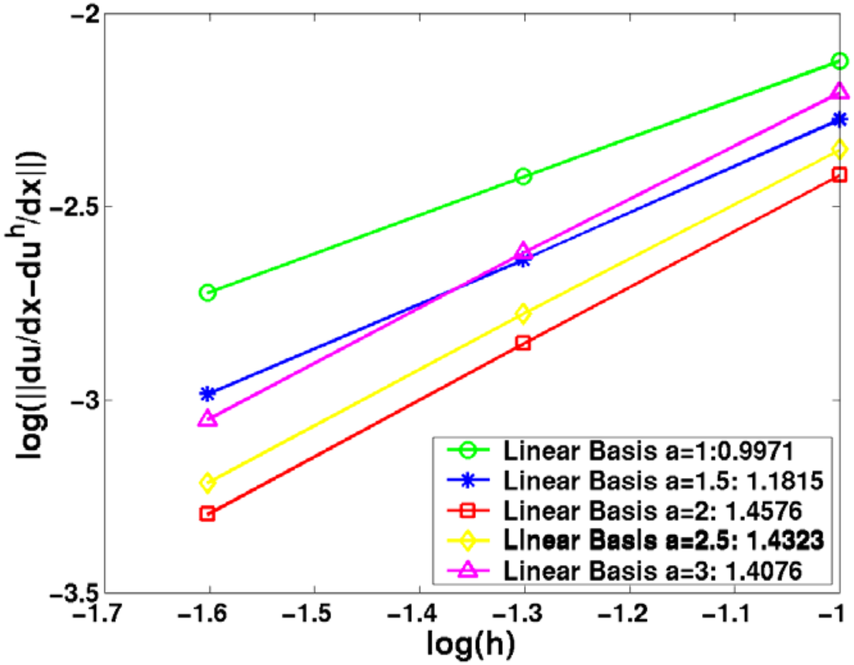

UCLA

Rank Instability in Direct Nodal Integration

Direct Nodal Integration: **4** zero eigenvalues

3 zero eigenvalues: Rigid Body Modes

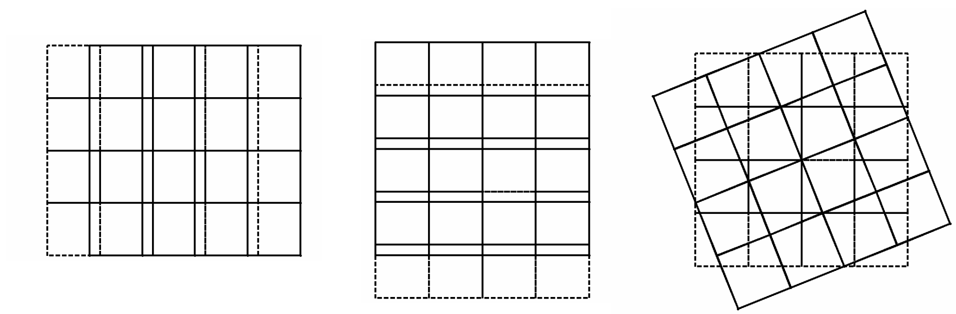

4th zero eigenvalue: spurious zero energy mode

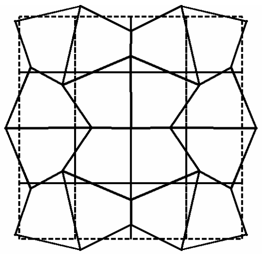

$$u_{,xx} = 10x$$

$$u(0) = u(1) = 0$$

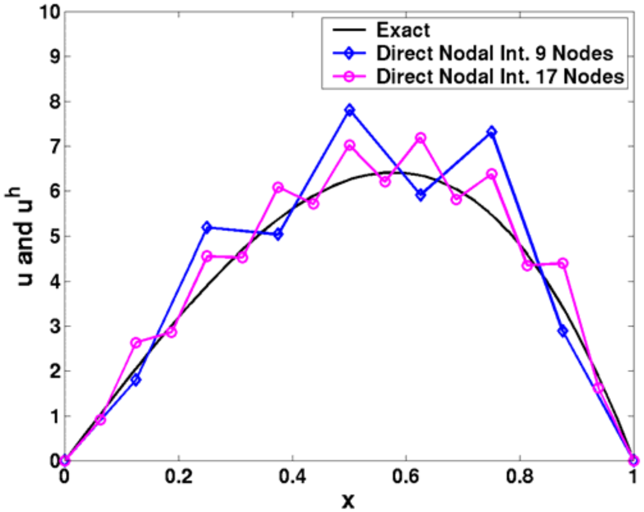

Stabilized Conforming Nodal Integration (SCNI)

Linear Patch Test Requirements

Linear Consistency $\sum_I \phi_I(\boldsymbol{x}) = 1, \quad \sum_I \phi_I(\boldsymbol{x}) x_{jI} = x_j$

Integration Constraints $\hat{\int_\Omega} \nabla \phi_I(\boldsymbol{x}) d\Omega = \hat{\int_{\partial\Omega}} \phi_I(\boldsymbol{x}) \boldsymbol{n} d\Gamma$

Stabilized Conforming Nodal Integration (SCNI)

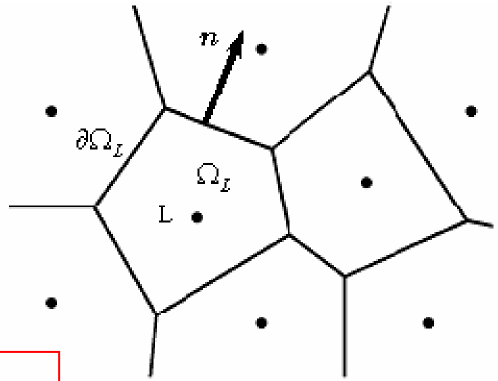

Gradient Smoothing

$$\bar{\nabla} u^h(\mathbf{x}_L) = \frac{1}{w_L}\int_{\Omega_L} \nabla u^h d\Omega = \frac{1}{w_L}\int_{\partial\Omega_L} u^h \boldsymbol{n} d\Gamma = \sum_{I=1}^{NP} \bar{\nabla}\phi_I(\mathbf{x}_L) u_I,$$

$$\bar{\nabla}\phi_I(\mathbf{x}_L) = \frac{1}{w_L}\int_{\partial\Omega_L} \phi_I \boldsymbol{n} d\Gamma \qquad \boxed{\Rightarrow \hat{\int_\Omega} \bar{\nabla}\phi_I(\mathbf{x}) d\Omega = \sum_{L=1}^{NP} \bar{\nabla}\phi_I(\mathbf{x}_L) w_L = \hat{\int_{\partial\Omega}} \phi_I(\mathbf{x}) \boldsymbol{n} d\Gamma}$$

(Linear Patch Test)

Nodal Integration $\bar{a}^h(\boldsymbol{v}^h, \boldsymbol{u}^h)_\Omega = (\boldsymbol{v}, \boldsymbol{t})_{\Gamma_t} \Rightarrow \boldsymbol{Kd} = \boldsymbol{f}$

$$\boldsymbol{K}_{IJ} = \sum_{L=1}^{NP} \bar{\nabla}^T \phi_I(\mathbf{x}_L) \bar{\nabla}\phi_J(\mathbf{x}_L) w_L$$

(Chen, Wu, Yoon, 2001)

UCLA

Eigenvalue Analysis

Direct Nodal Integration: **4** zero eigenvalues

3 zero eigenvalues: Rigid Body Modes

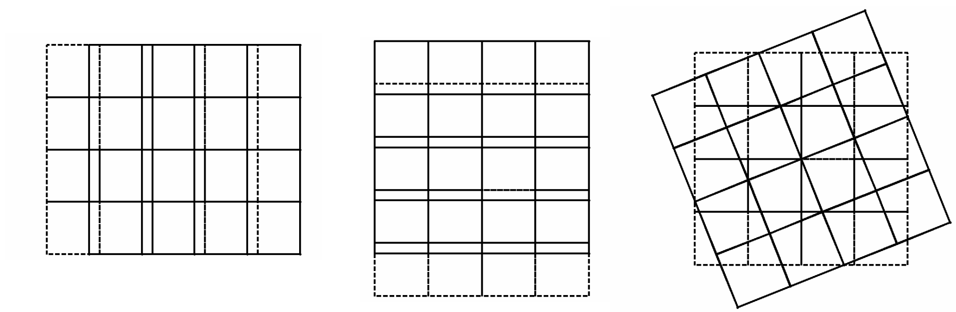

4th zero eigenvalue:
spurious zero energy mode

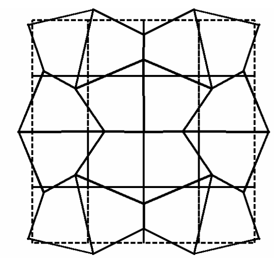

SCNI: **3** zero eigenvalues

3 zero eigenvalues: Rigid Body Modes

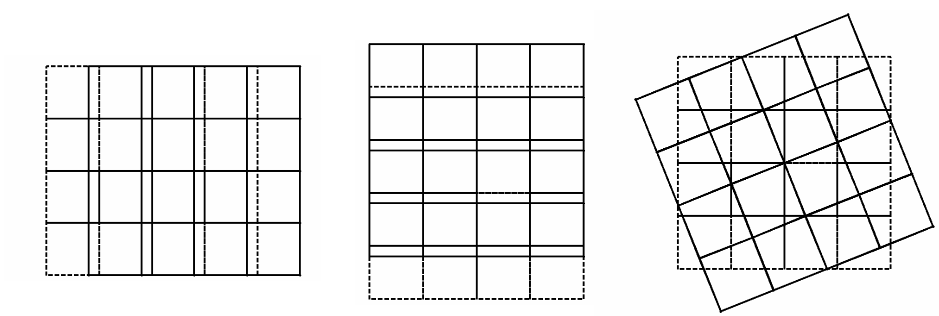

4th smallest eigenvalue:
deformation modes

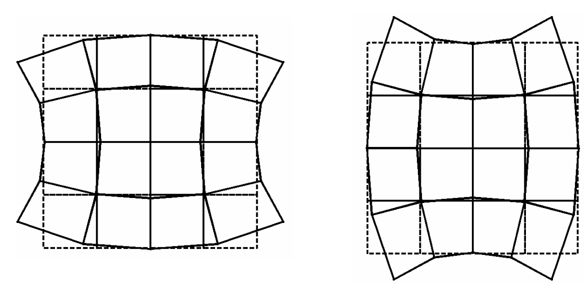

UCLA

$$u_{,xx} = x \qquad u(0) = u(1) = 0$$

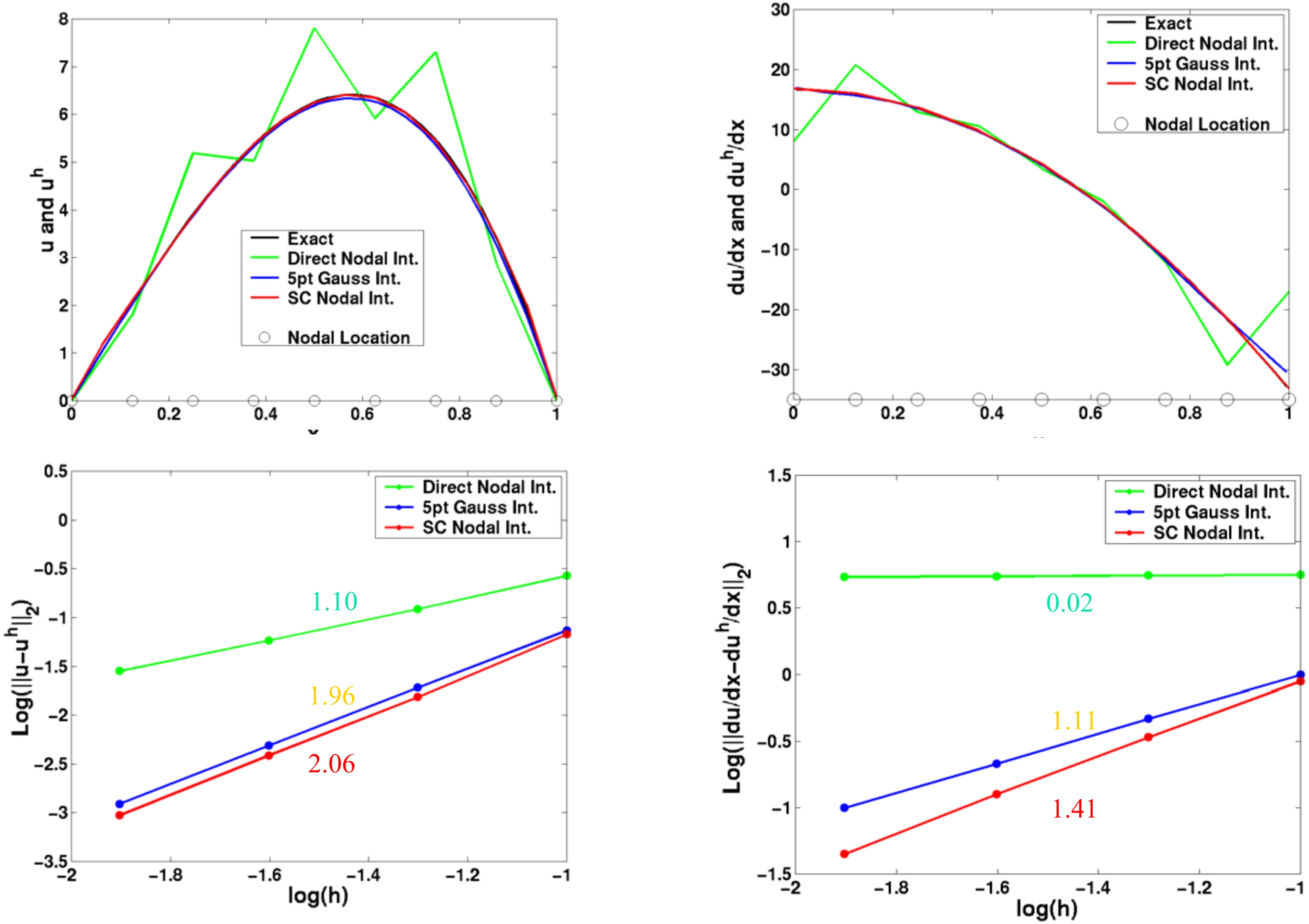

Stability of RKPM with SCNI and DNI

SCNI

DNI

Stable Material

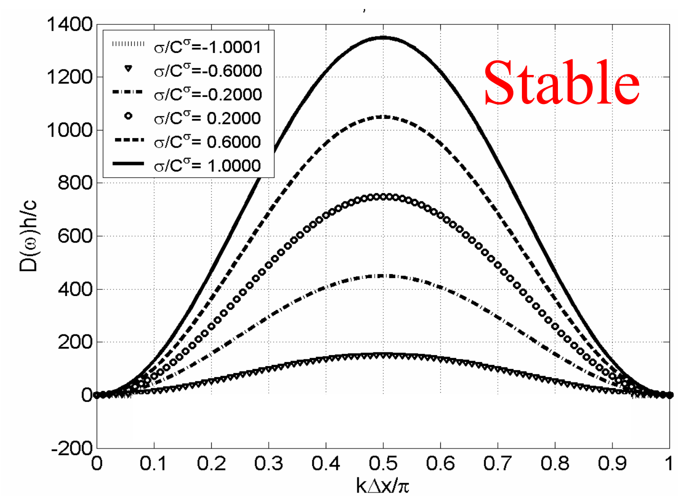

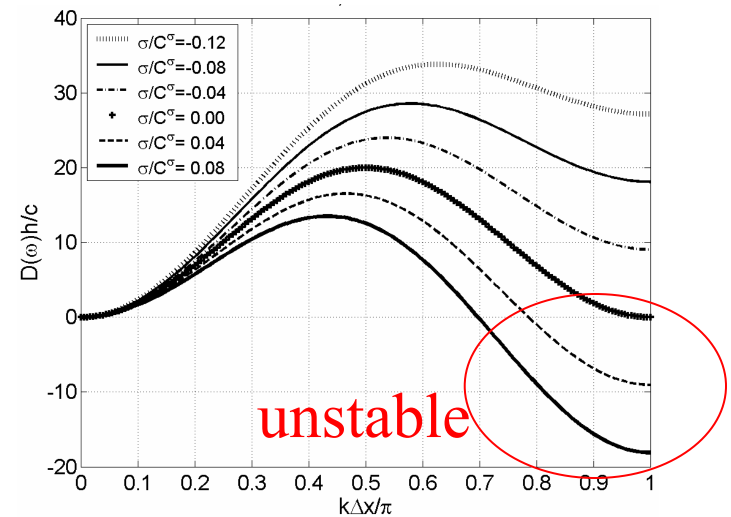

Material Instability (softening)

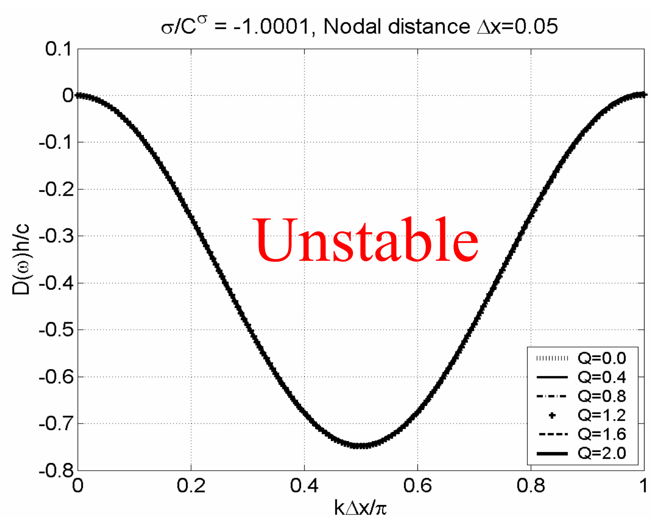

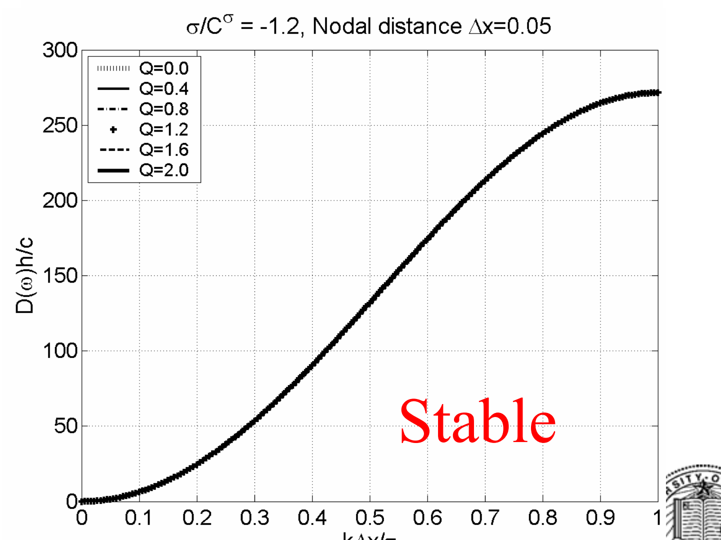

UCLA

Stability Analysis of Full Discrete Equation

Nodal Integration

$$c^2\Delta t^2 < \frac{1}{\left[\begin{array}{l}\Psi_{,x}^2(+2h)\sin^2(2kh)+\Psi_{,x}^2(+h)\sin^2(kh)\\ +4\Psi_{,x}(+h)\Psi_{,x}(+2h)\sin^2(kh)\cos(kh)\end{array}\right]}$$

Stabilized Conforming Nodal Integration

$$\frac{c^2\Delta t^2}{h^2} < \frac{1}{\left[\begin{array}{l}\Psi^2\left(\frac{1}{2}h\right)\sin^2(kh)\\ +2\Psi^2\left(\frac{3}{2}h\right)\sin^2\left(\frac{kh}{2}\right)\left[1+\cos(3kh)\right]\\ +4\Psi\left(\frac{1}{2}h\right)\Psi\left(\frac{3}{2}h\right)\sin^2\left(\frac{kh}{2}\right)\left[\begin{array}{l}\cos(2kh)\\ +\cos(kh)\end{array}\right]\end{array}\right]}$$

Stabilized non-Conforming Nodal Integration

$$\frac{c^2\Delta t^2}{h^2} < \frac{\alpha^2}{\left[\begin{array}{l}\Psi^2\left(\left(2-0.5\alpha\right)h\right)\sin^2(2kh)\\ +\Psi^2\left(\left(1-0.5\alpha\right)h\right)\sin^2(kh)\\ +4\Psi\left(\left(2-0.5\alpha\right)h\right)\Psi\left(\left(1-0.5\alpha\right)h\right)\sin^2(kh)\cos(kh)\end{array}\right]}$$

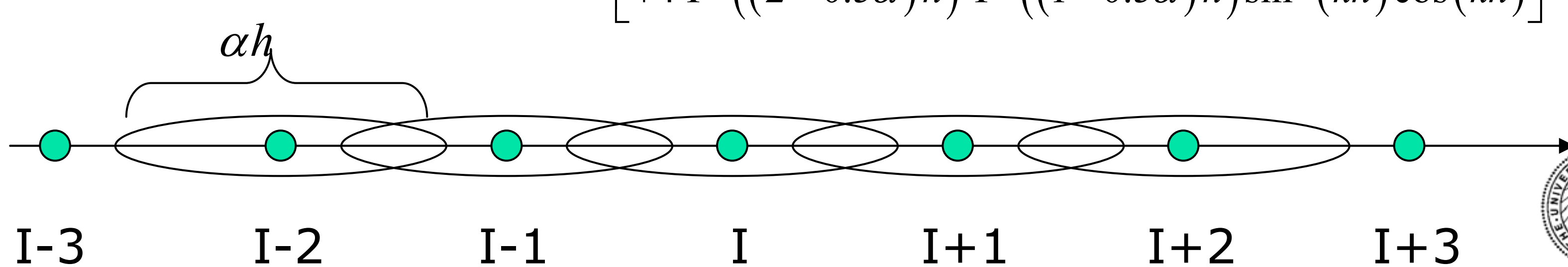

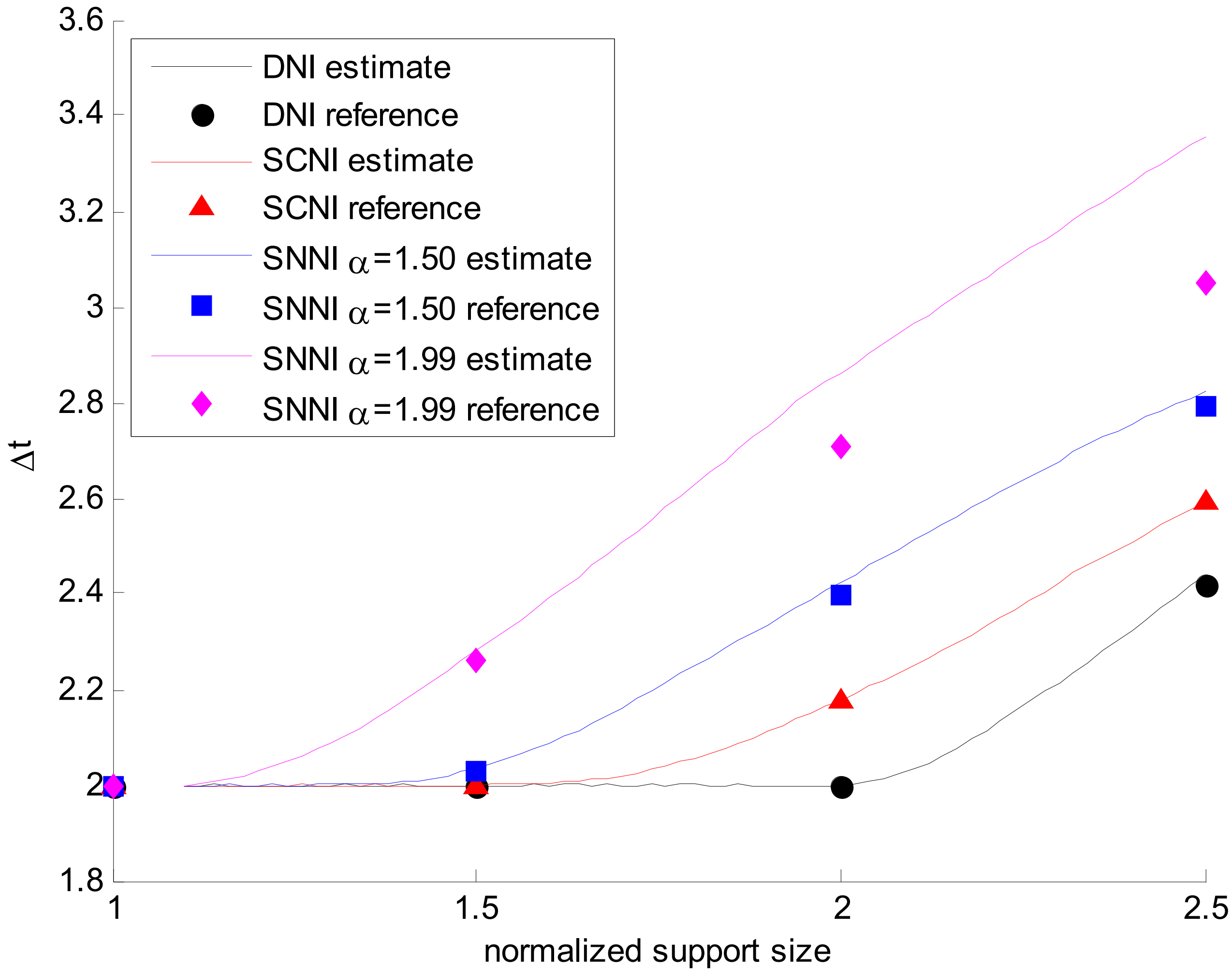
DNI estimate
DNI reference
SCNI estimate
SCNI reference
SNNI α=1.50 estimate
SNNI α=1.50 reference
SNNI α=1.99 estimate
SNNI α=1.99 reference
Δt
normalized support size
3.6
3.4
3.2
3
2.8
2.6
2.4
2.2
2
1.8
1
1.5
2
2.5

Challenging Problems for FEM

Large Deformation

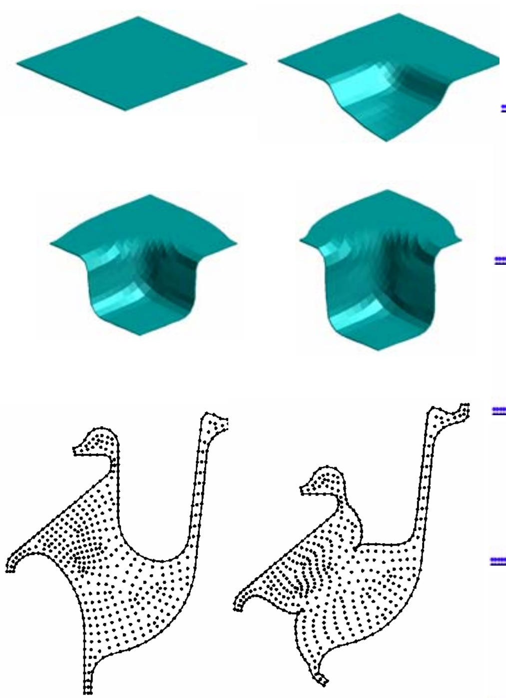

Damage & Failure

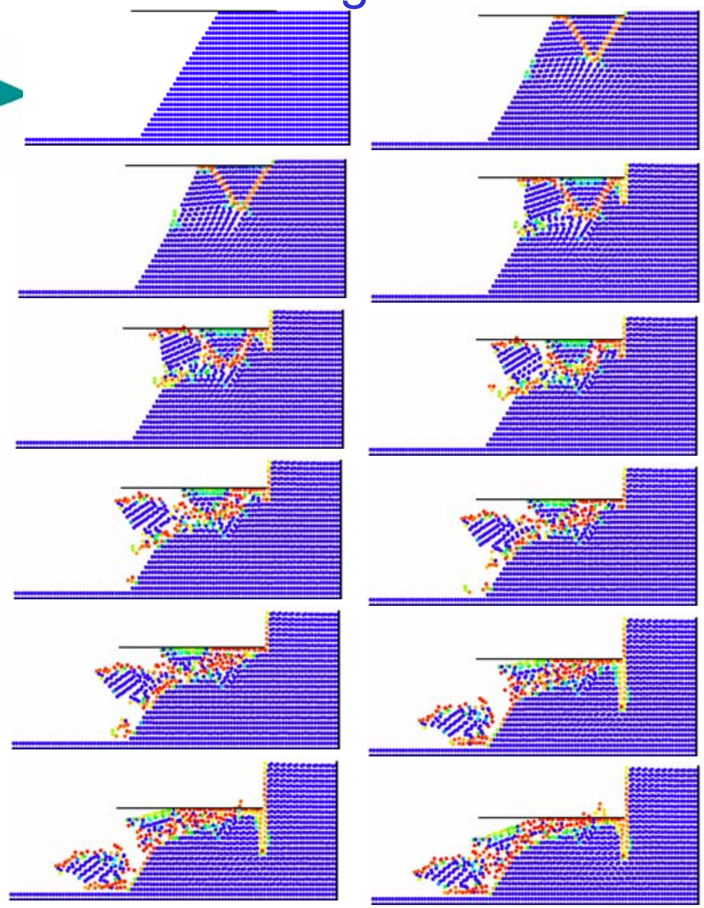

Microstructural Evolution

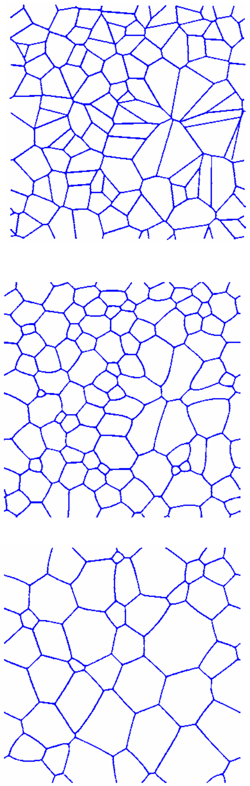

Singularity

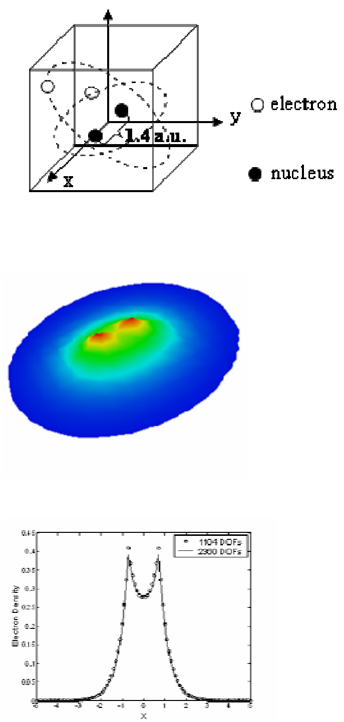

Earth Excavation

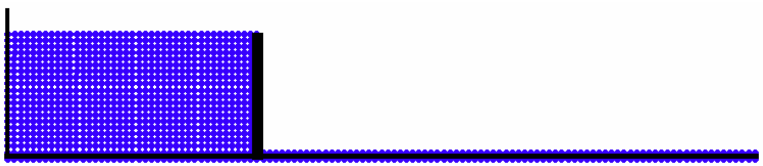

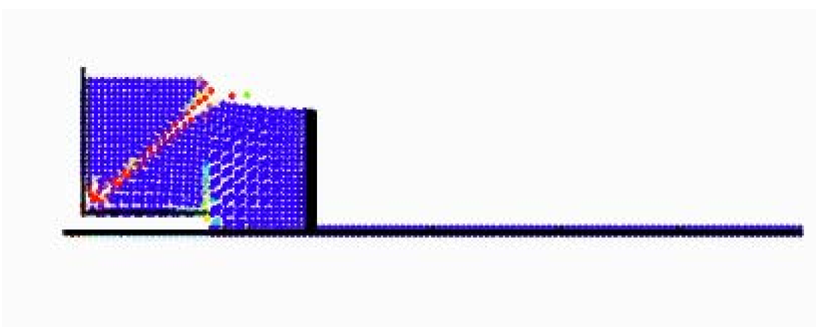

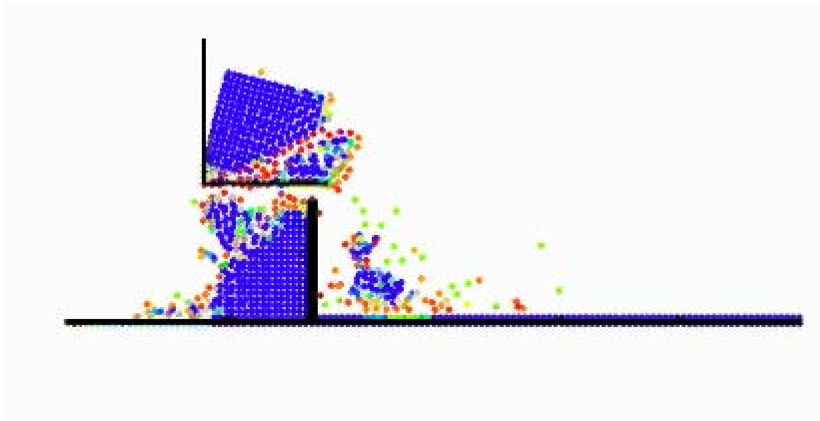

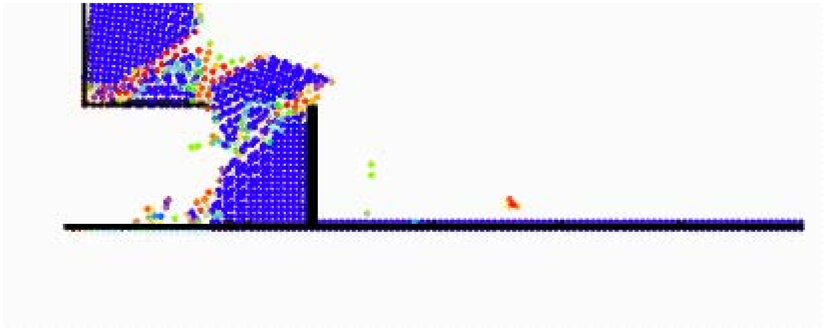

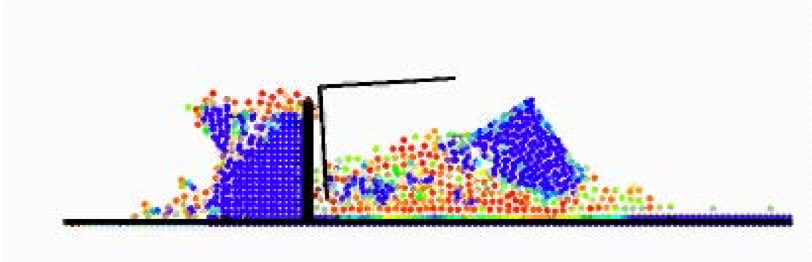

Animation

UCLA

Coupled RKPM-FEM Earth Moving Simulation

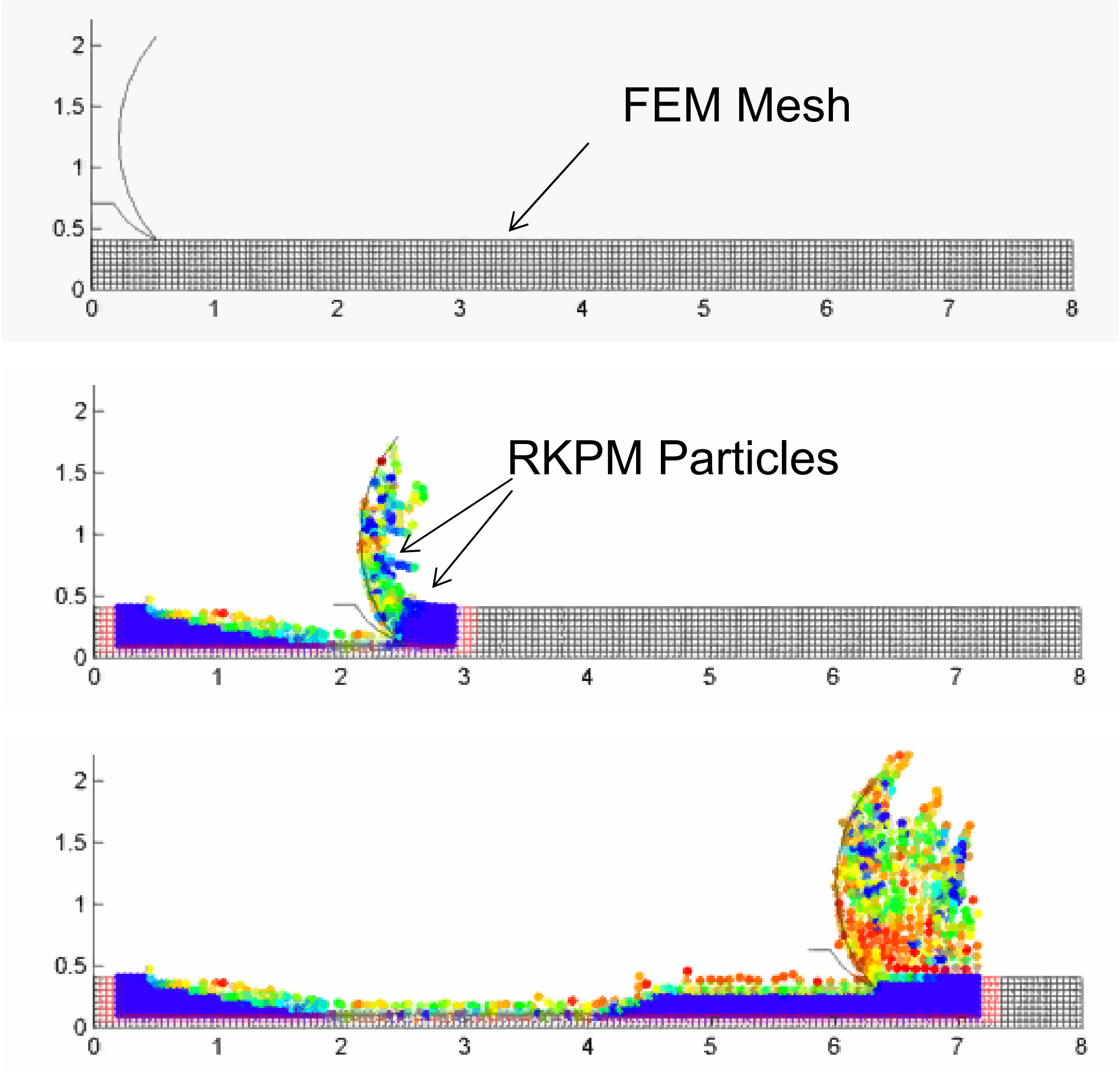

Animation

3D Adaptive Penetration Simulation (30°)

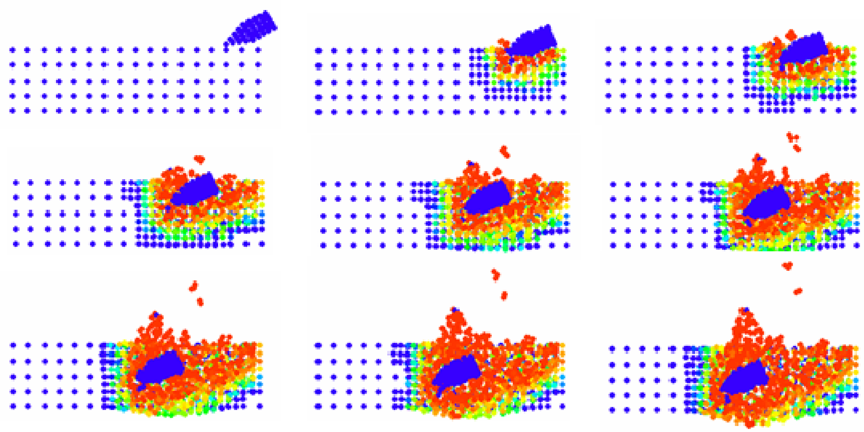

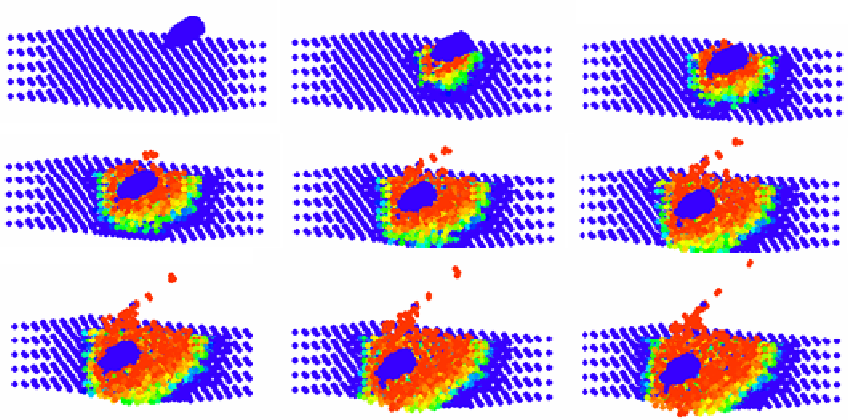

Animation

Animation (Angle View)

Penetration of Steel Plate

Movie1 Movie2

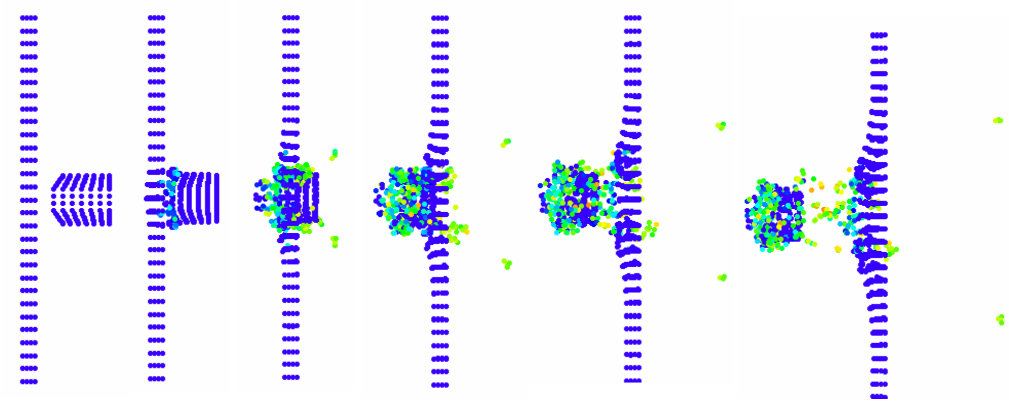

	Numerical	Experimental
Exit velocity	2440 ft/sec	2437 ft/sec

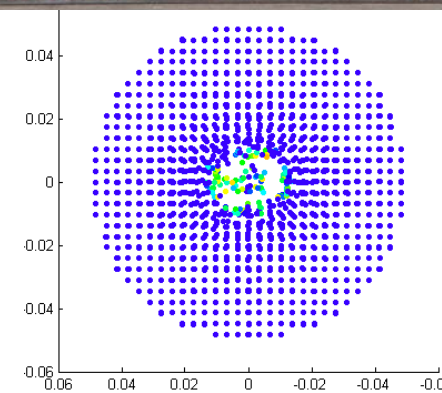

Numerical result : 2.1 cm = 0.82 inch

Experimental result : 0.82 inch

UCLA

Multi-scale Materials Modeling

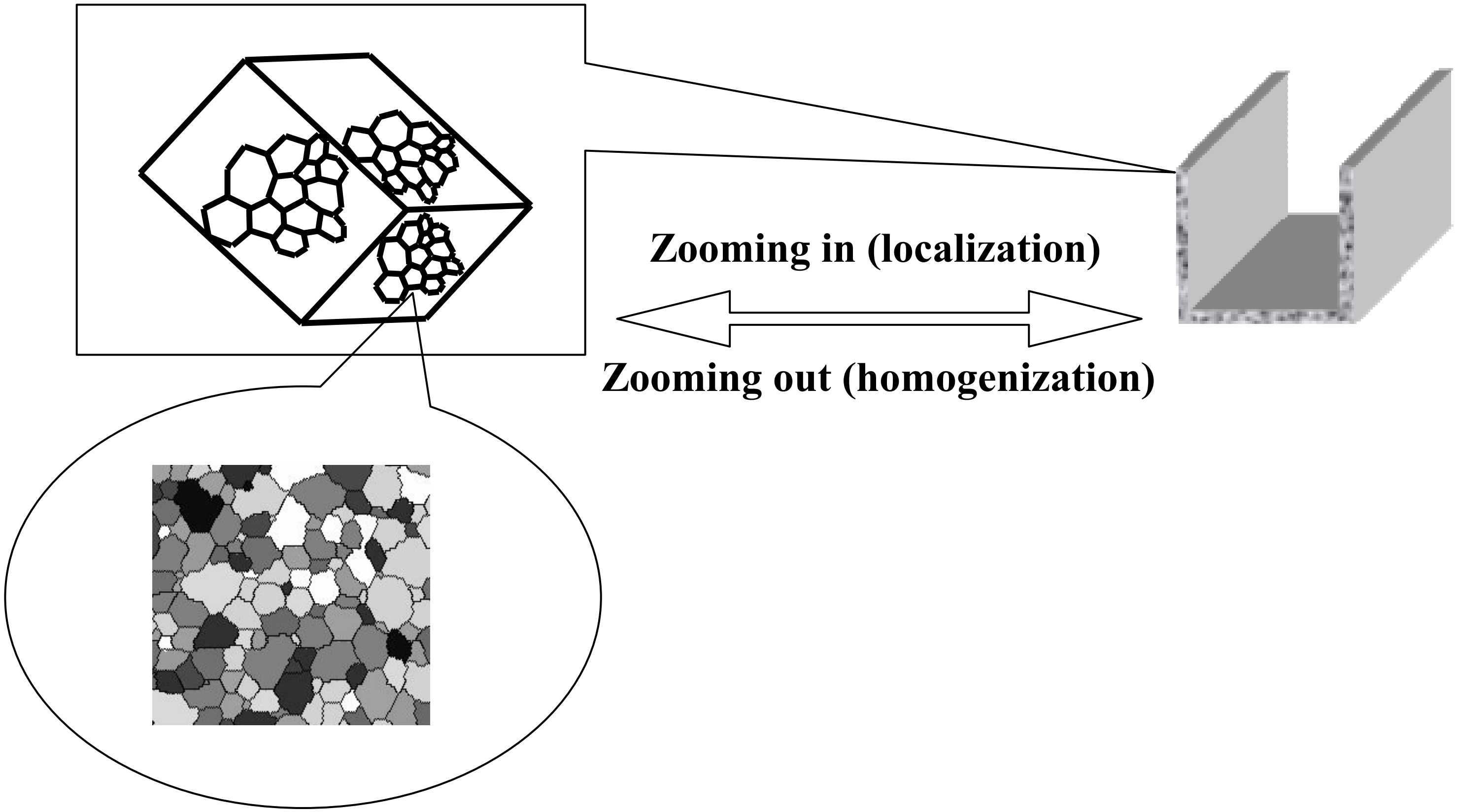

Multi-scale Asymptotic Expansion

- Macro & meso coordinates relations:

$$\mathbf{y} = \begin{pmatrix} y_1 \\ y_2 \\ y_3 \end{pmatrix}, \quad \mathbf{x} = \begin{pmatrix} x_1 \\ x_2 \\ x_3 \end{pmatrix} \rightarrow \mathrm{y_i} = \frac{\mathrm{x_i}}{\lambda}$$

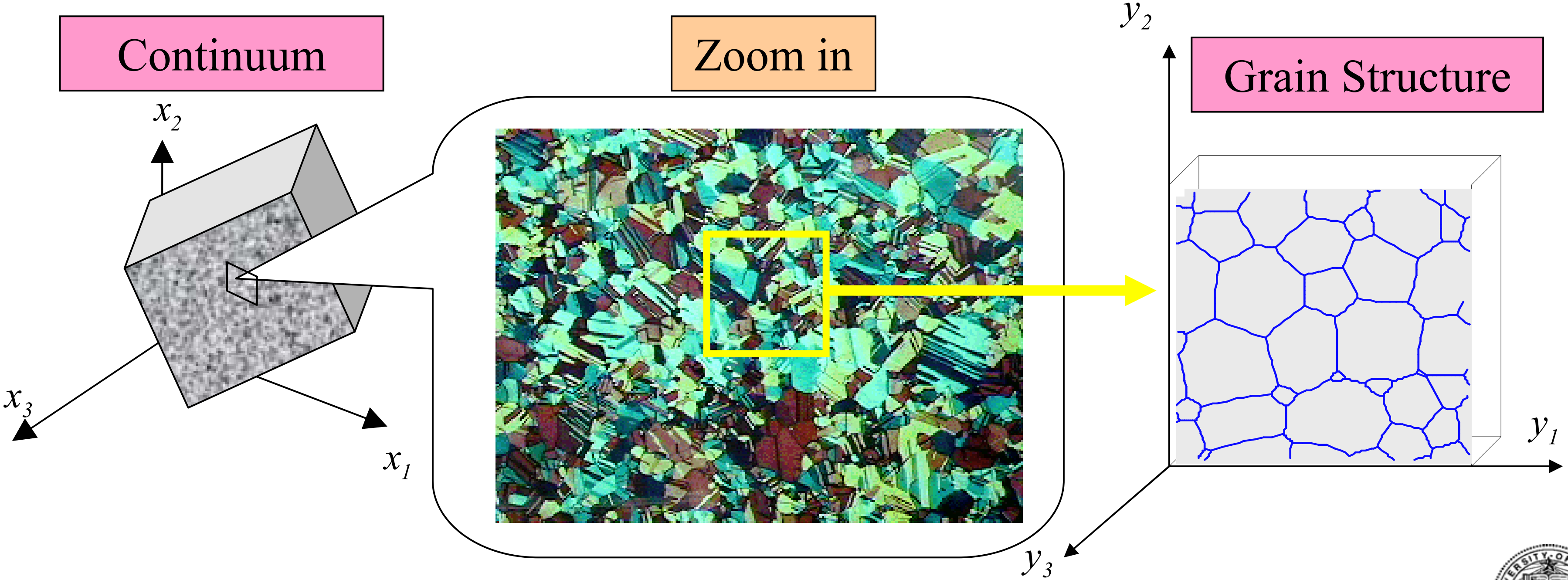

Basic Equations in Stressed Grain Growth

- **Variational Formulation of Grain Growth Dynamics**
  - Energy dissipation

$$\boxed{\delta \dot{W}_1 = \int_{\Gamma_{gb}} f_c \delta \bar{v}_n d\Gamma_{gb} = \int_{\Gamma_{gb}} \frac{\bar{v}_n}{m} \delta \bar{v}_n d\Gamma_{gb}}$$

  - Grain boundary tension

$$\boxed{\delta \dot{W}_2 = \int_{\Gamma_{gb}} \gamma \delta \dot{\varepsilon}_s ds = \int_{\Gamma_{gb}} \gamma \left(\frac{\delta \bar{v}_n}{R} + \frac{\partial \delta \bar{v}_s}{\partial s}\right) ds}$$

  - Strain energy effect

$$\boxed{\delta \dot{W}_3 = \int_{\Gamma_{gb}} \frac{1}{2}\left(\boldsymbol{\sigma}^+ : \boldsymbol{\varepsilon}^+ - \boldsymbol{\sigma}^- : \boldsymbol{\varepsilon}^-\right) \delta \bar{v}_n d\Gamma + \int_{\Omega} \delta \dot{\boldsymbol{\varepsilon}} : \boldsymbol{C} : \dot{\boldsymbol{\varepsilon}} d\Omega}$$

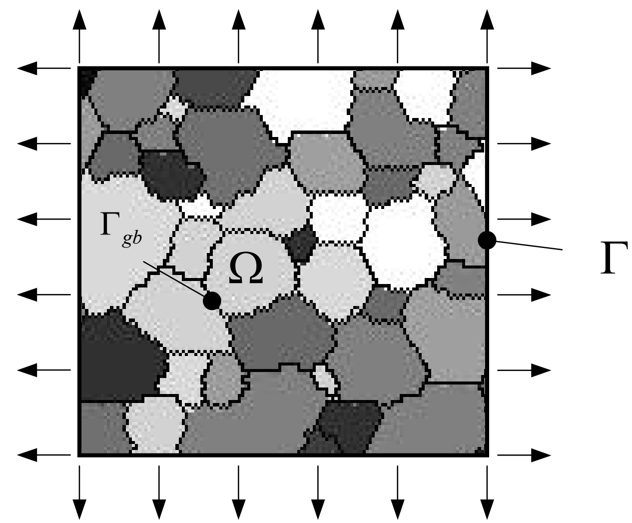

  - Variational Equation

Meso-scale

Meso-Macro scale

Macro scale

$$\boxed{\int_{\Gamma_{gb}} \gamma \left(\frac{\partial \delta \bar{v}_s}{\partial s} + \frac{\delta \bar{v}_n}{R}\right) ds + \int_{\Gamma_{gb}} \frac{\bar{v}_n}{m} \delta \bar{v}_n ds}$$

$$+ \boxed{\int_{\Gamma_{gb}} \delta \bar{v}_n \frac{1}{2}\left(\boldsymbol{\sigma}^+ : \boldsymbol{\varepsilon}^+ - \boldsymbol{\sigma}^- : \boldsymbol{\varepsilon}^-\right) d\Gamma + \int_{\Omega} \delta \dot{\boldsymbol{\varepsilon}} : \boldsymbol{C} : \dot{\boldsymbol{\varepsilon}} d\Omega} - \left(\boxed{\int_{\Gamma_h} \delta \boldsymbol{v} \cdot \boldsymbol{h} d\Gamma + \int_{\Omega} \delta \boldsymbol{v} \cdot \boldsymbol{b} d\Gamma} \right) = 0$$

UCLA

Scale Decomposition of Virtual Power

Grain deformation velocity $$v_i = v_i(\mathbf{x},\mathbf{y}) = v_i^{[0]}(\mathbf{x},\mathbf{y}) + \lambda v_i^{[1]}(\mathbf{x},\mathbf{y}) + O(\lambda^2)$$

Grain boundary velocity $$\bar{v}_i = \bar{v}_i(\mathbf{x},\mathbf{y}) = \bar{v}_i^{[0]}(\mathbf{x},\mathbf{y}) + \lambda \bar{v}_i^{[1]}(\mathbf{x},\mathbf{y}) + O(\lambda^2)$$

- Strain rate decomposition

$$\dot{\varepsilon} = \nabla^s \boldsymbol{v}$$

$$\begin{aligned}\dot{\varepsilon}_{ij} &= \frac{1}{\lambda}\left(\dot{\varepsilon}_{ij}^{[0]}\right) + \left(\dot{\varepsilon}_{ij}^{[0]} + \dot{\varepsilon}_{ij}^{[1]}\right) + \lambda\left(\dot{\varepsilon}_{ij}^{[1]} + \dot{\varepsilon}_{ij}^{[2]}\right) + \lambda^2\left(\dot{\varepsilon}_{ij}^{[2]} + \dot{\varepsilon}_{ij}^{[3]}\right) + \cdots \\ &= \lambda^{-1}\dot{\varepsilon}_{ij}^{[-1]} + \lambda^0\dot{\varepsilon}_{ij}^{[0]} + \lambda\dot{\varepsilon}_{ij}^{[1]} + \lambda^2\dot{\varepsilon}_{ij}^{[2]} + \cdots\end{aligned}$$

- Stress decomposition

$$\sigma_{ij}^{[n]} = c_{ijkl}\dot{\varepsilon}_{kl}^{[n]}$$

$$\sigma_{ij} = \lambda^{-1}\sigma_{ij}^{[-1]} + \lambda^0\sigma_{ij}^{[0]} + \lambda\sigma_{ij}^{[1]} + \lambda^2\sigma_{ij}^{[2]} + \cdots$$

Scale Decomposition of Virtual Power

Resultant asymptotic expansion of virtual power

$$\delta\Pi(\boldsymbol{v}^0+\lambda\boldsymbol{v}^{[1]},\overline{\boldsymbol{v}}^{[0]}+\lambda\overline{\boldsymbol{v}}^{[1]})=\lambda^{-2}\left(\delta\Pi^{[-2]}\right)+\lambda^{-1}\left(\delta\Pi^{[-1]}\right)+\lambda^{0}\left(\delta\Pi^{[0]}\right)+O(l^1)=0$$

1. Leading order equation for coarse scale solution $O\left(\lambda^{-2}\right)$**:**

$$\int_\Omega \frac{1}{2}\delta\left(\dot{\varepsilon}_{ij}^{[-1]}\sigma_{ij}^{[-1]}\right)\,d\Omega=0 \;\Rightarrow\; \boxed{\frac{\partial\sigma_{ij}^{[-1]}}{\partial y_j}=0} \;\Rightarrow\; \boxed{v_i^{[0]}(x,y)=v_i^{[0]}(x)}$$

2. Leading order equation for coupling function $O\left(\lambda^{-1}\right)$ **:**

$$\int_\Omega \frac{1}{2}\delta\left(\dot{\varepsilon}_{ij}^{[-1]}\sigma_{ij}^{[0]}+\dot{\varepsilon}_{ij}^{[0]}\sigma_{ij}^{[-1]}\right)\,d\Omega=0 \;\Rightarrow\; \boxed{\frac{\partial\sigma_{ij}^{[0]}}{\partial y_j}+\frac{\partial\sigma_{ij}^{[-1]}}{\partial x_j}=0} \;\Rightarrow\; \boxed{v_k^{[1]}=\alpha_{kmn}(y)\,\dot{\varepsilon}_{mn}^{[0]}(x)}$$

3. Leading order equation for fine scale $O\left(\lambda^{0}\right)$ **:**

(1) $$\int_\Omega \frac{1}{2}\delta\left(\dot{\varepsilon}_{ij}^{[-1]}:\sigma_{ij}^{[1]}+\dot{\varepsilon}_{ij}^{[0]}:\sigma_{ij}^{[0]}+\dot{\varepsilon}_{ij}^{[1]}:\sigma_{ij}^{[-1]}\right)\,d\Omega+\int_{\Gamma_h}\delta\boldsymbol{v}^{[0]}\cdot\boldsymbol{h}\,d\Gamma+\int_\Omega \delta\boldsymbol{v}^{[0]}\cdot\boldsymbol{b}\,d\Gamma=0$$

$$\Rightarrow\; \boxed{\begin{cases}\dfrac{\partial\sigma_{ij}^{[0]}}{\partial x_j}+\dfrac{\partial\sigma_{ij}^{[1]}}{\partial y_j}+b_i=0 & \text{in}\quad \Omega,\ i=1,2,3\\[2ex] \boldsymbol{\sigma}^{[0]}\cdot\boldsymbol{n}=\boldsymbol{h} & \text{on}\quad \Gamma_h\end{cases}} \;\Rightarrow\; \boxed{\overline{C}_{ijmn}=\frac{1}{S}\int_{\Omega^y}C_{ijkl}\left(I_{klmn}+\frac{1}{2}\left(\frac{\partial\alpha_{imn}}{\partial y_j}+\frac{\partial\alpha_{jmn}}{\partial y_i}\right)\right)d\Omega}$$

UCLA

Grain Boundary Velocity Decomposition

(2) $$\delta \prod_{gb}(\boldsymbol{v},\overline{\boldsymbol{v}}) = \int_{\Gamma_{gb}} \frac{1}{2}\left(\sigma_{ij}^{+}\varepsilon_{ij}^{+} - \sigma_{ij}^{-}\varepsilon_{ij}^{-}\right)\delta\overline{v}_n \, \mathrm{d}\Gamma + \int_{\Gamma_{gb}} \gamma\left(\frac{\partial\delta\overline{v}_s}{\partial s} + \frac{\delta\overline{v}_n}{R}\right)\mathrm{d}\Gamma + \int_{\Gamma_{gb}} \frac{\delta\overline{v}_n}{\mu}\overline{v}_n \mathrm{d}\Gamma = 0$$

Scale Decomposition:

Coarse scale $\left(\overline{v}_n^{[0]}\right)$:

$$\int_{\Omega^y} \frac{1}{2}\left[\varepsilon_{ij}^{+[0]}\sigma_{ij}^{+[0]} - \varepsilon_{ij}^{-[0]}\sigma_{ij}^{-[0]}\right]\delta\overline{v}_n^{[0]}\mathrm{d}\Gamma + \int_{\Gamma_{gb}^y} \gamma\left(\frac{\partial\delta\overline{v}_s^{[0]}}{\partial s} + \frac{\delta\overline{v}_n^{[0]}}{R}\right)\mathrm{d}\Gamma + \int_{\Gamma_{gb}^y} \frac{\delta\overline{v}_n^{[0]}}{\mu}\overline{v}_n^{[0]}\mathrm{d}\Gamma = 0$$

Fine scale $\left(\overline{v}_n^{[1]}\right)$:

$$\int_{\Omega^y} \frac{1}{2}\left[\varepsilon_{ij}^{+[0]}\sigma_{ij}^{+[1]} + \varepsilon_{ij}^{+[1]}\sigma_{ij}^{+[0]} - \varepsilon_{ij}^{-[0]}\sigma_{ij}^{-[1]} - \varepsilon_{ij}^{-[1]}\sigma_{ij}^{-[0]}\right]\delta\overline{v}_n^{[1]}\mathrm{d}\Gamma + \int_{\Gamma_{gb}^y} \frac{\delta\overline{v}_n^{[1]}}{\mu}\overline{v}_n^{[1]}\mathrm{d}\Gamma = 0$$

Approximation of Coarse and Fine Scale Solutions

Multi-scale Variables:

1. Coarse-fine scale coupling function
2. Grain boundary velocity
3. Material velocity

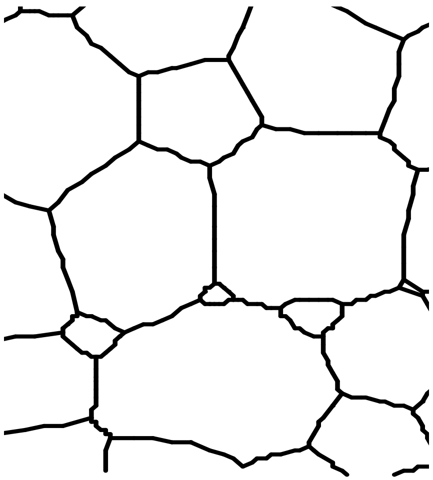

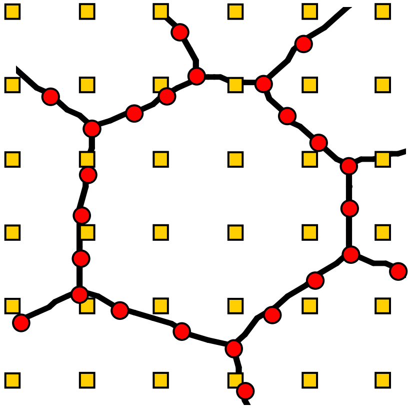

- Grain interior point
- Grain boundary point

- Grain boundary migration velocity

$$\bar{v}_i(s,t) = \sum_I N_I(s)\bar{v}_{iI}(t)$$

$N_I(s)$: finite element shape function

- Coarse-fine coupling function

$$\alpha_{ijk}(\boldsymbol{x},t) = \sum_I \Psi_I(\boldsymbol{x})\alpha_{ijkI}(t)$$

$\Psi_I(\boldsymbol{x})$: Meshfree shape function

UCLA

Grain Boundary Interface Conditions

$$\alpha_{ijk}(\boldsymbol{x}) = \sum_{I=1}^{NP} \Psi_I(\boldsymbol{x})\alpha_{ijkI} + \sum_{I=1}^{NS} \hat{\Psi}_I(\boldsymbol{x})\hat{\alpha}_{ijkI}$$

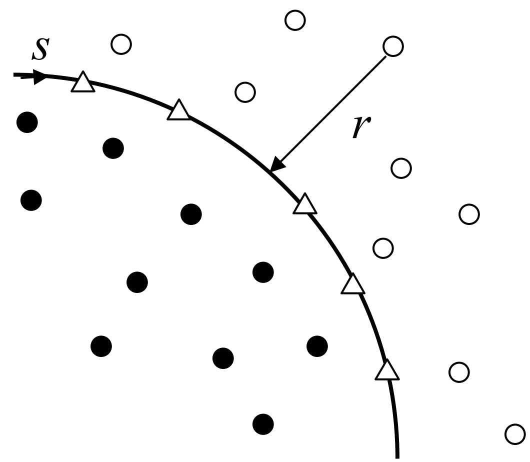

$\hat{\Psi}_I(\boldsymbol{x})$: interface enrichment function

$$\hat{\Psi}_I(\boldsymbol{x}) = \varphi(r)\phi_I(s)$$

$$\frac{\partial \varphi}{\partial r} \in C^{-1}$$

$\Psi_I(\boldsymbol{x})$: Smooth shape function

$$\Psi_I(\boldsymbol{x}) = \boldsymbol{H}^T(\boldsymbol{x} - \boldsymbol{x}_I)\boldsymbol{b}(\boldsymbol{x})\Phi_I(\boldsymbol{x} - \boldsymbol{x}_I)$$

$$\boldsymbol{H}^T(\boldsymbol{x} - \boldsymbol{x}_I) = [1, x_1 - x_{1I}, x_2 - x_{2I}]$$

Coupling: $\sum_I [\Psi_I(\boldsymbol{x}) + \hat{\Psi}_I(\boldsymbol{x})] x_{1I}^i x_{2I}^j = x_1^i x_2^j \qquad i + j = 0,1$

$$\Psi_I(\boldsymbol{x}) = \boldsymbol{H}^T(\boldsymbol{x} - \boldsymbol{x}_I)\boldsymbol{M}^{-1}(\boldsymbol{x})[\boldsymbol{H}(\boldsymbol{0}) - \hat{\boldsymbol{F}}(\boldsymbol{x})]\Phi_a(\boldsymbol{x} - \boldsymbol{x}_I)$$

$$\hat{\boldsymbol{F}}(\boldsymbol{x}) = \sum_{I=1}^{NS} \hat{\Psi}_I(\boldsymbol{x})\boldsymbol{H}(\boldsymbol{x} - \boldsymbol{x}_I)$$

Modeling of Microstructural Evolution

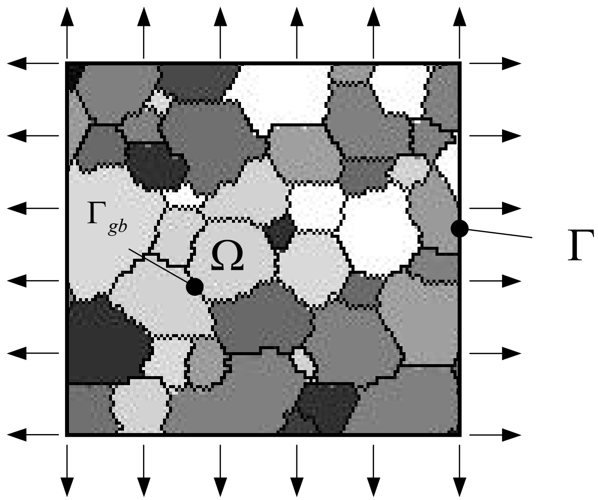

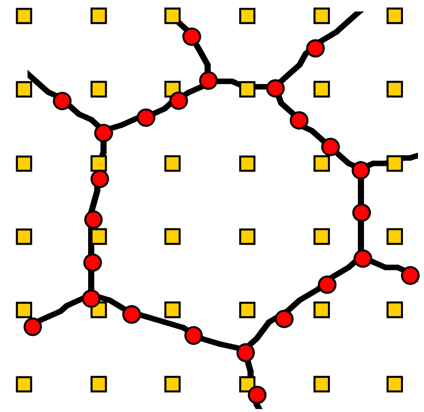

Grain interior point

Grain boundary point

Interface Enrichment Function

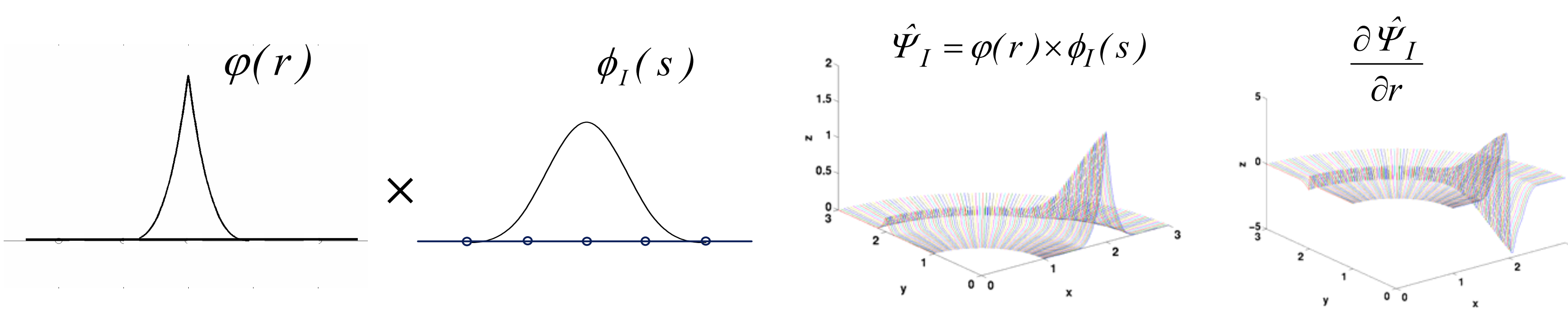

Level Set Simulation of Grain Growth

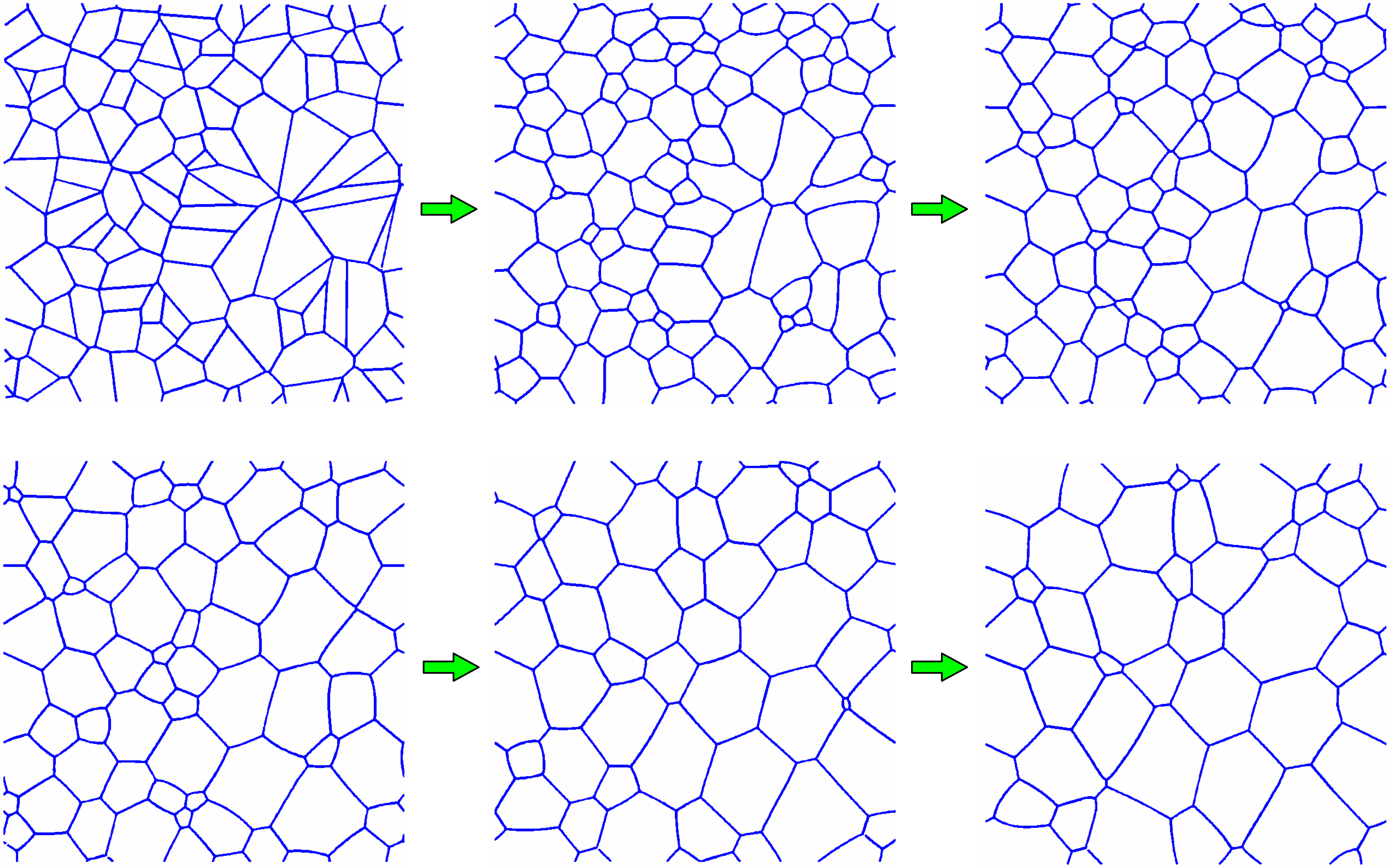

DNA: Segment of Double Strands DNA

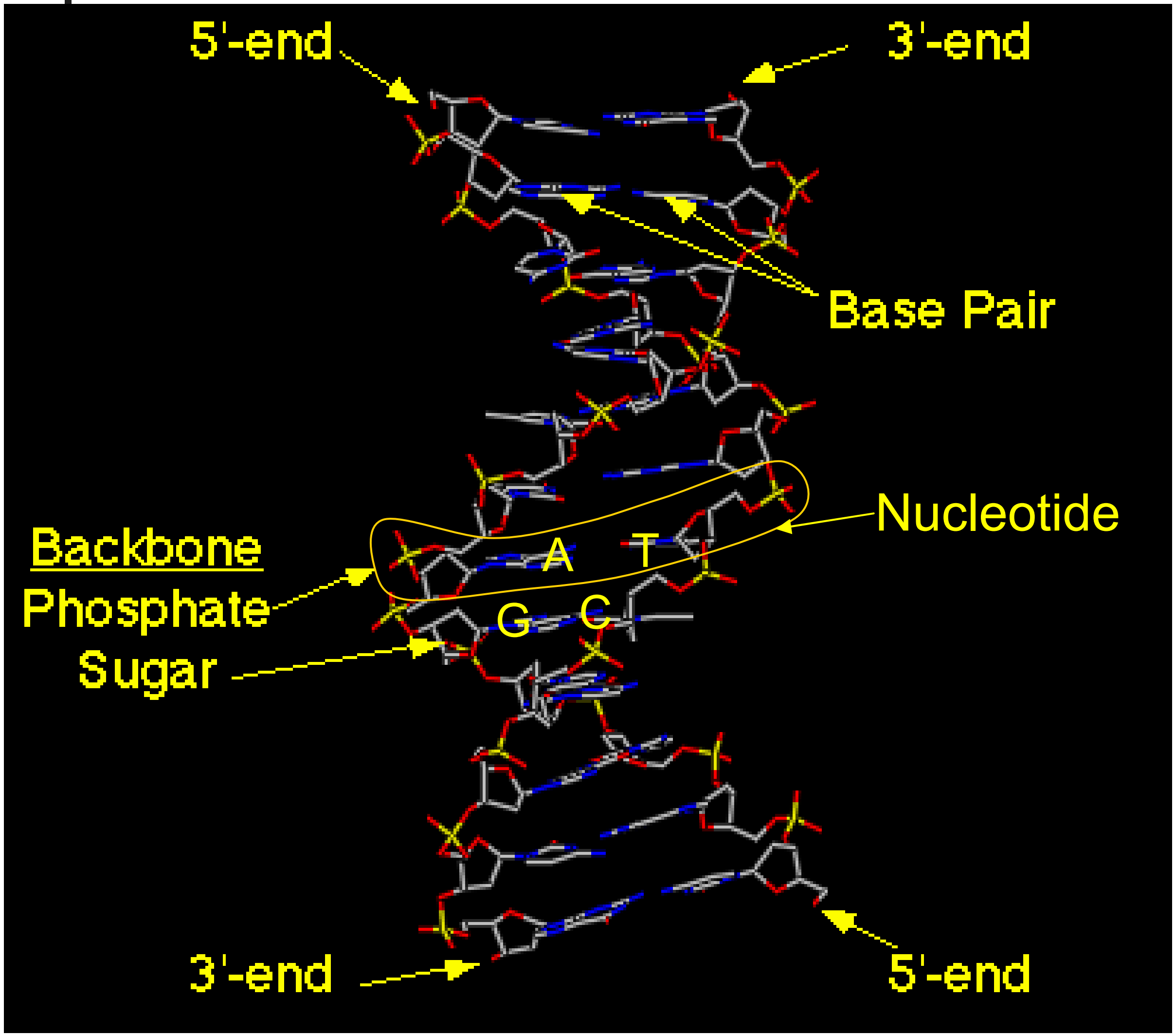

First-level Multi-scale Homogenization

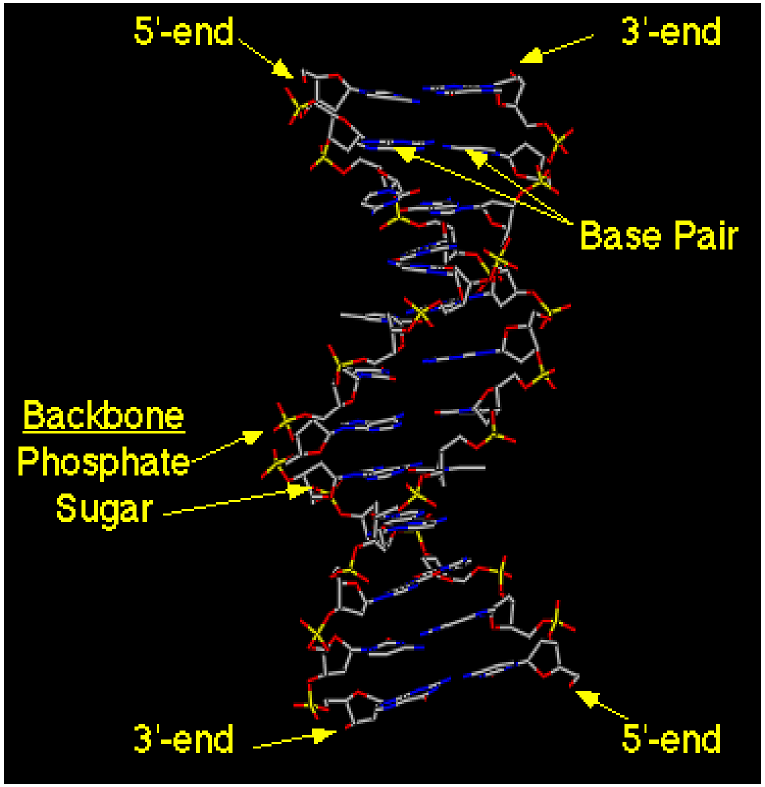

DNA Molecule

$$\begin{array}{ccccccc} & & \tilde{u}^{n-1} & & \tilde{u}^{n-2} & & \tilde{u}^{n-3} & \cdots \\ \boxed{Q_n} & \nearrow & \boxed{Q_{n-1}} & \nearrow & \boxed{Q_{n-2}} & \nearrow & & \\ \bar{u}^{n} & \rightarrow & \bar{u}^{n-1} & \rightarrow & \bar{u}^{n-2} & \rightarrow & \bar{u}^{n-3} & \rightarrow \cdots \\ & \boxed{P_n} & & \boxed{P_{n-1}} & & \boxed{P_{n-2}} & & \end{array}$$

$$\boldsymbol{w}_j \boldsymbol{U}_{j+1} = \begin{bmatrix} \boldsymbol{Q}_j \\ \boldsymbol{P}_j \end{bmatrix} \boldsymbol{U}_{j+1} = \begin{bmatrix} \boldsymbol{U}^h_{j+1} \\ \boldsymbol{U}^l_{j+1} \end{bmatrix}$$

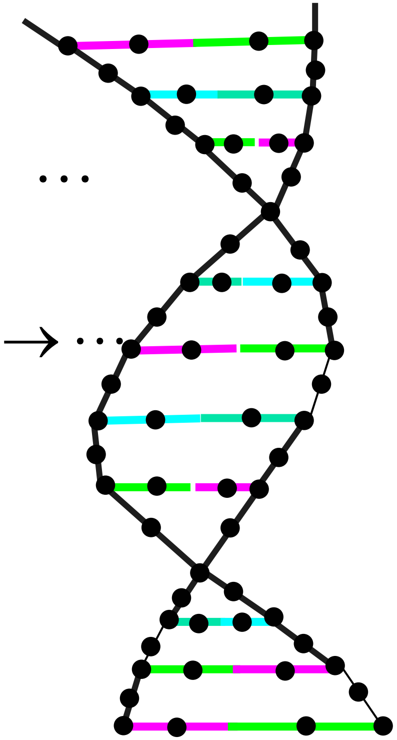

Coarse-Grained Model

Multi-scale wavelet projection of potential function

Wavelet Based Multi-scale Homogenization

$$\cdots \subset V_{-1} \subset V_0 \subset V_1 \subset \cdots \subset L^2(R)$$ (Sequence of nested subspaces)

$$\overline{\bigcup_{j\in\mathbb{Z}} V_{-j}} = L^2(R)$$

$$\bigcap_{j\in\mathbb{Z}} V_j = \{0\}$$

$$V_j = V_{j-1} \oplus W_{j-1}$$ (Mutually orthogonal spaces)

Scaling function: $\phi^*(x) \in V_j \Leftrightarrow \phi^*(2x) \in V_{j+1}, \quad j \in \mathbb{Z}$

Wavelet: $\psi^*(x) \in W_j \Leftrightarrow \psi^*(2x) \in W_{j+1}, \quad j \in \mathbb{Z}$

(Scaling law)

$$\phi^*(x) \in V_j \Leftrightarrow \phi^*(x-n) \in V_j, \text{ for all } n \in \mathbb{Z}$$

$$\psi^*(x) \in W_j \Leftrightarrow \psi^*(x-n) \in W_j, \text{ for all } n \in \mathbb{Z}$$

(Translation law)

UCLA

Homogenization & Localization

Scaling function

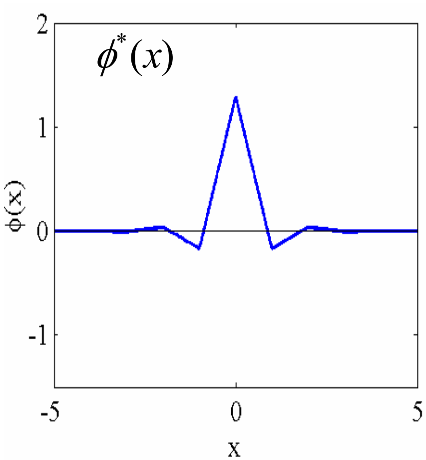

Wavelet

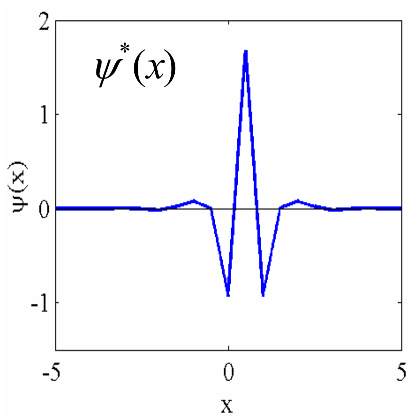

$$\begin{tikzcd}
 & \tilde{u}^{n-1} & \tilde{u}^{n-2} & \tilde{u}^{n-3} & \cdots \\
\bar{u}^{n} \arrow[r, "P_n"'] \arrow[ur, "Q_n"] & \bar{u}^{n-1} \arrow[r, "P_{n-1}"'] \arrow[ur, "Q_{n-1}"] & \bar{u}^{n-2} \arrow[r, "P_{n-2}"'] \arrow[ur, "Q_{n-2}"] & \bar{u}^{n-3} \arrow[r] & \cdots
\end{tikzcd}$$

$$w_j U_{j+1} = \begin{bmatrix} Q_j \\ P_j \end{bmatrix} U_{j+1} = \begin{bmatrix} U^h_{j+1} \\ U^l_{j+1} \end{bmatrix}$$

$$\begin{tikzcd}
\cdots & \tilde{u}^{n-3} \arrow[dr, "w^{-1}_{n-2}"'] & \tilde{u}^{n-2} \arrow[dr, "w^{-1}_{n-1}"'] & \tilde{u}^{n-1} \arrow[dr, "w^{-1}_{n}"'] & \\
\cdots \arrow[r] & \bar{u}^{n-3} \arrow[r] & \bar{u}^{n-2} \arrow[r] & \bar{u}^{n-1} \arrow[r] & \bar{u}^{n}
\end{tikzcd}$$

Coarse Graining of Basic Building Blocks

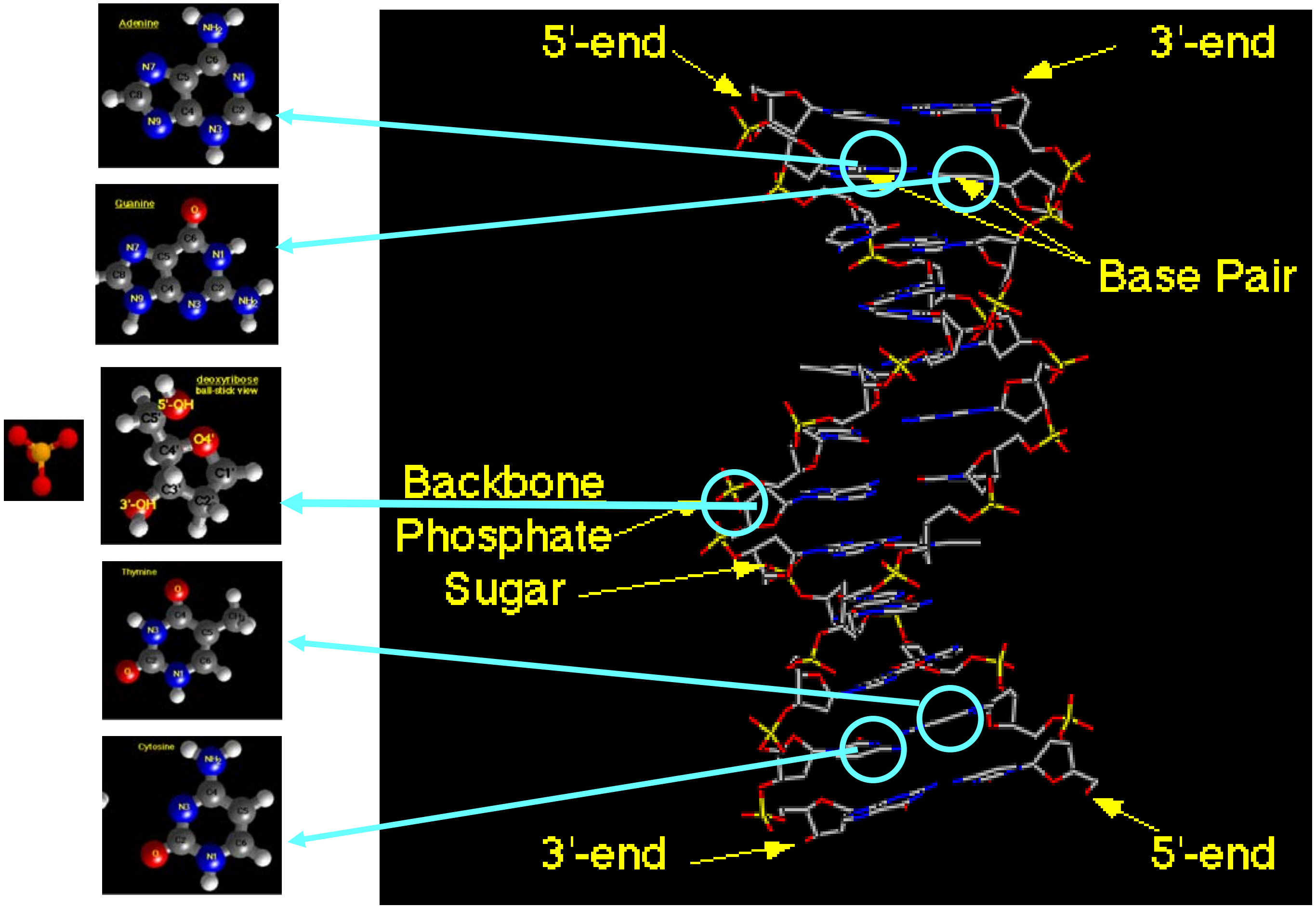

Coarse Graining of DNA Molecule

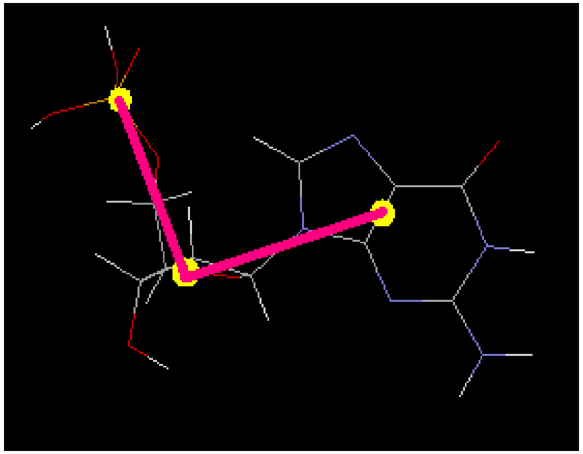

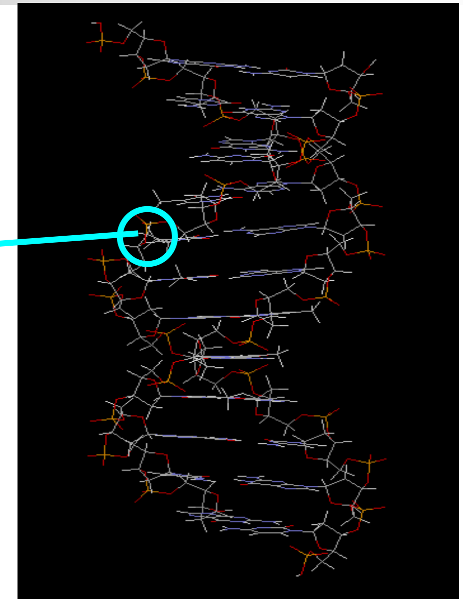

Collect atomistic distributions

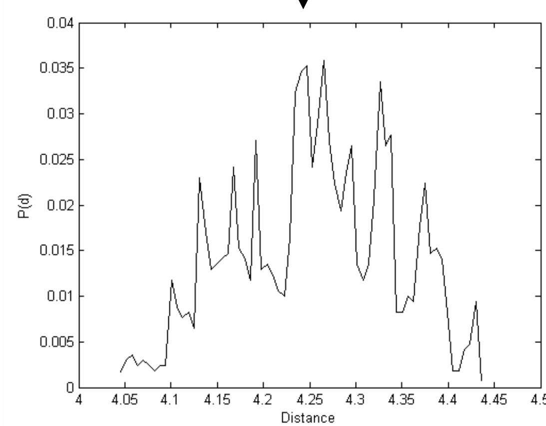

Fine-scale Distance Distribution (probability)

$$\boxed{U(d) = -k_B T \ln P(d)}$$

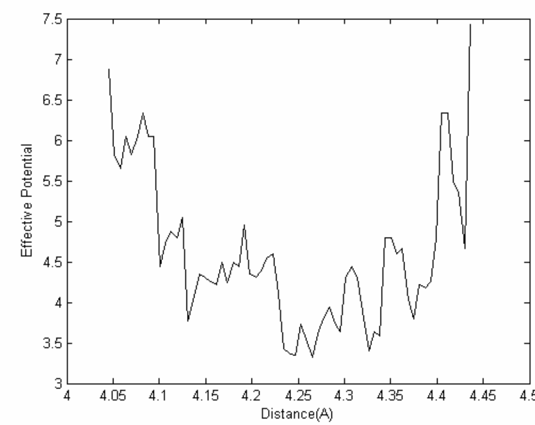

Fine-scale Potential

UCLA

Coarse Graining of DNA Molecule

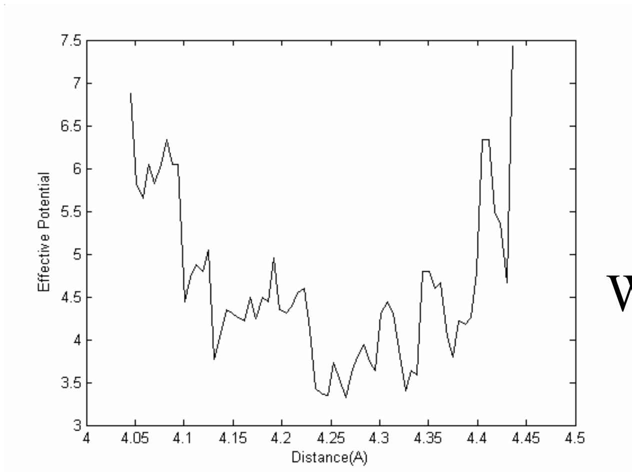

Wavelet Projection

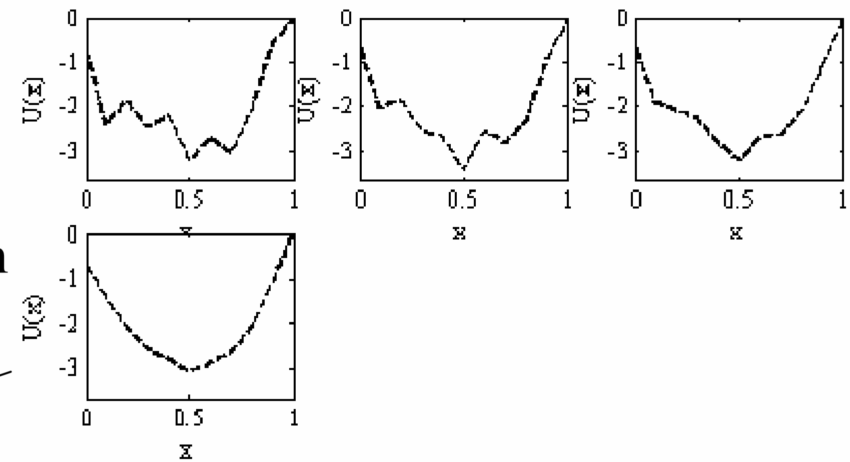

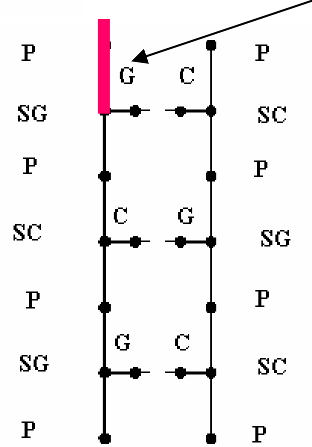

Characterize the Coarse-grained Parameters for Potential

$$U_{bond} = k_b (r_{ij} - r_{eq})^2$$

DNA Stretching by Coarse Grained Model

DNA Stretching: Molecular model

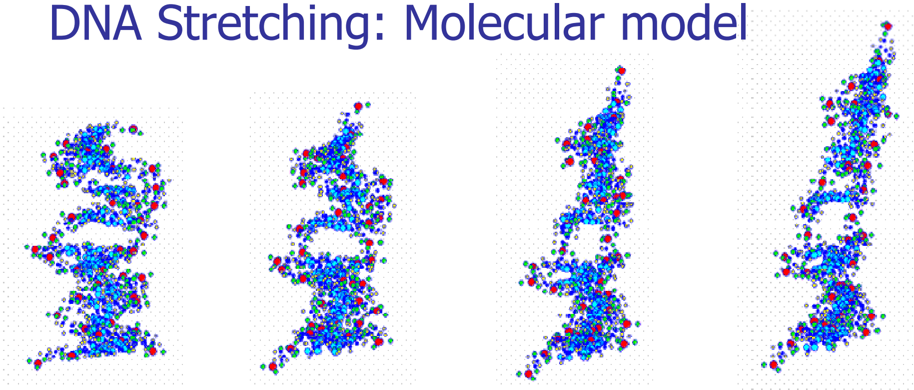

DNA Stretching: Coarse scale model

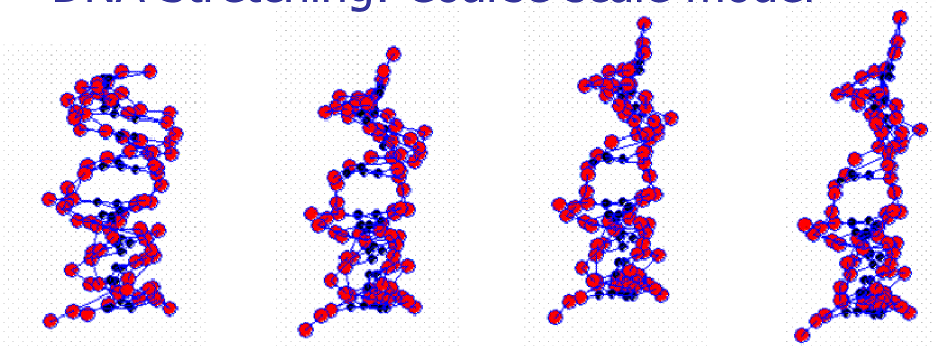

CPU= 1000:1

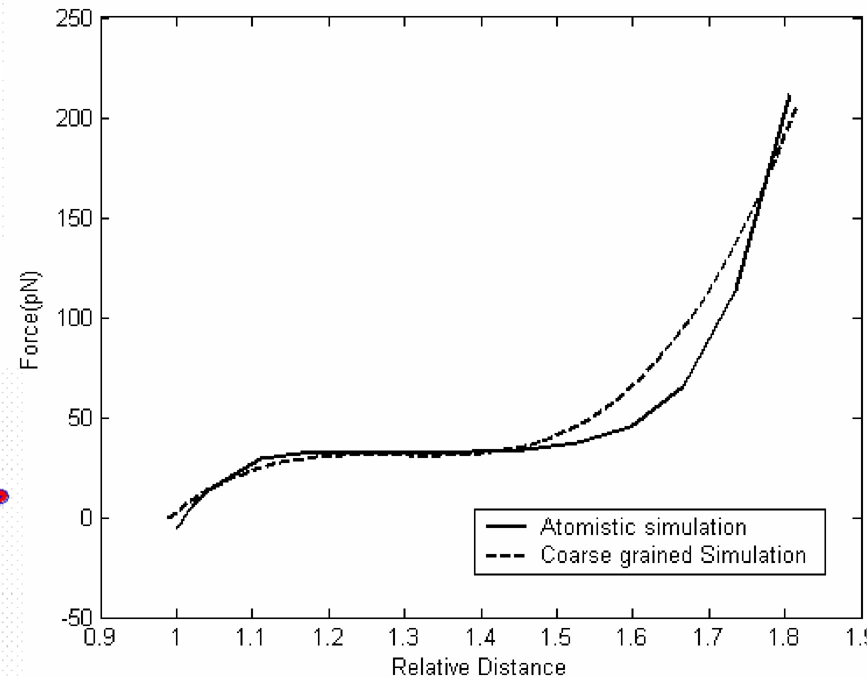

Second-level Multi-scale Homogenization

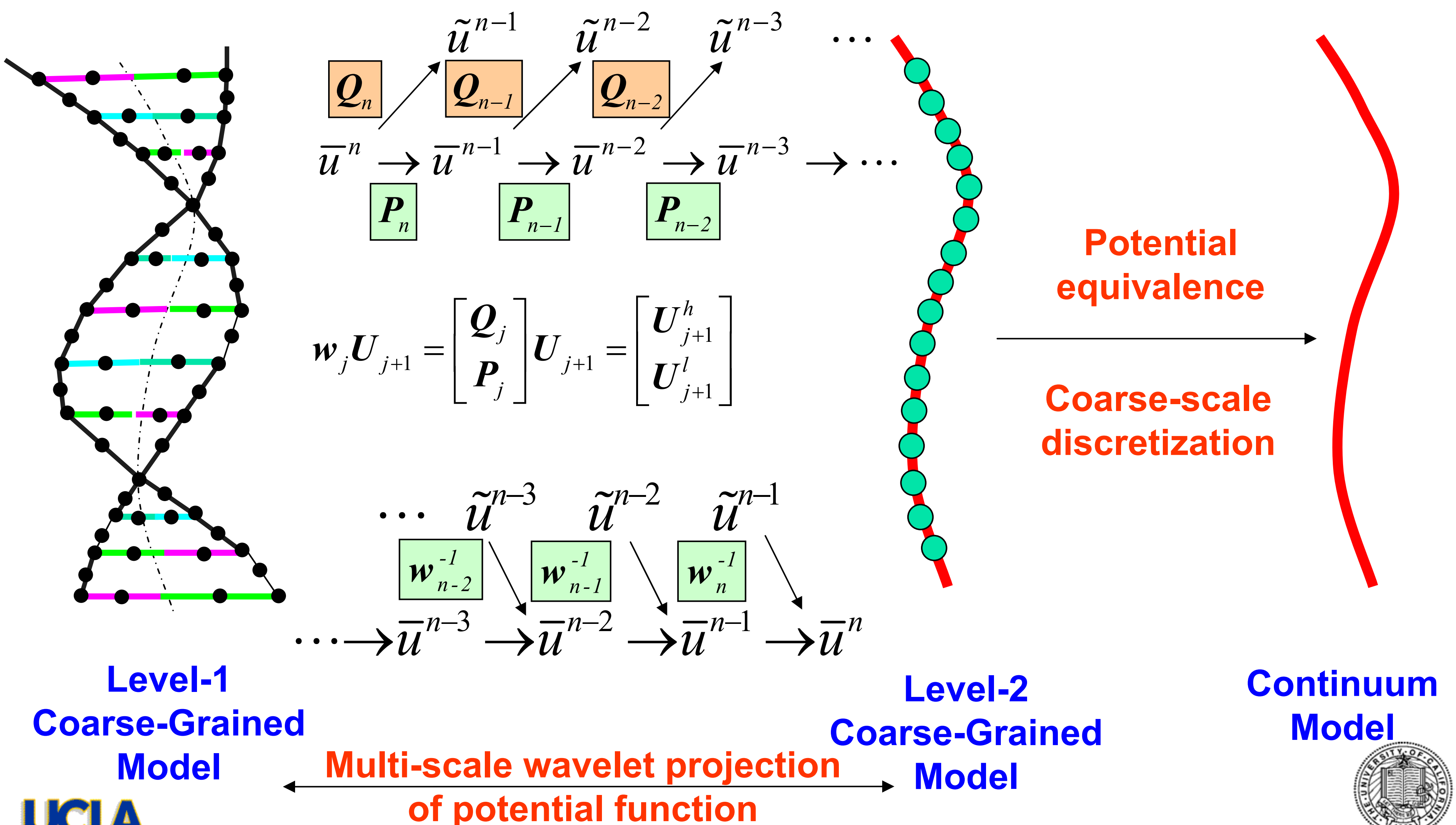

Second Level Homogenization of DNA Molecule

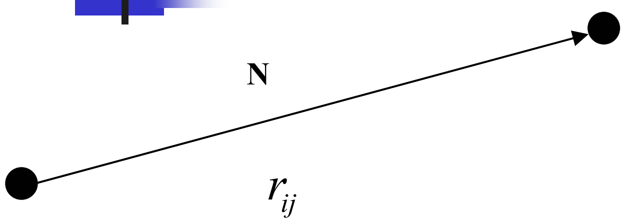

Bond energy

$$U^{bond} = \sum_{bonds} k_b (r_{ij} - r_{ij0})^2$$

$$\frac{r_{ij}}{r_{ij0}} = \sqrt{\mathbf{N} \bullet \mathbf{C} \bullet \mathbf{N}} = \sqrt{1 + 2\mathbf{N} \bullet \mathbf{E} \bullet \mathbf{N}}$$

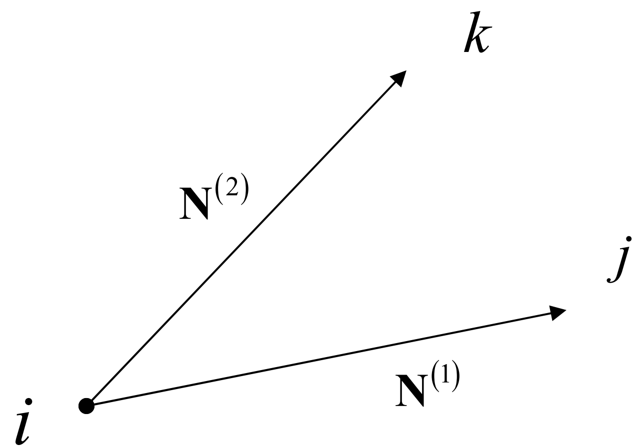

Bond energy

$$U_{ang} = \sum_{angles} k_\theta (\theta - \theta^0)^2$$

$$\cos\theta^0 = \mathbf{N}^{(1)} \bullet \mathbf{N}^{(2)}$$

$$\cos\theta = \frac{\mathbf{N}^{(1)} \bullet \mathbf{C} \bullet \mathbf{N}^{(2)}}{\sqrt{\mathbf{N}^{(1)} \bullet \mathbf{C} \bullet \mathbf{N}^{(1)}}\sqrt{\mathbf{N}^{(2)} \bullet \mathbf{C} \bullet \mathbf{N}^{(2)}}}$$

The 2nd PK stress

$$\mathbf{S}_{bond} = \frac{\partial U^{bond}}{\partial \mathbf{E}}$$

UCLA

Validation

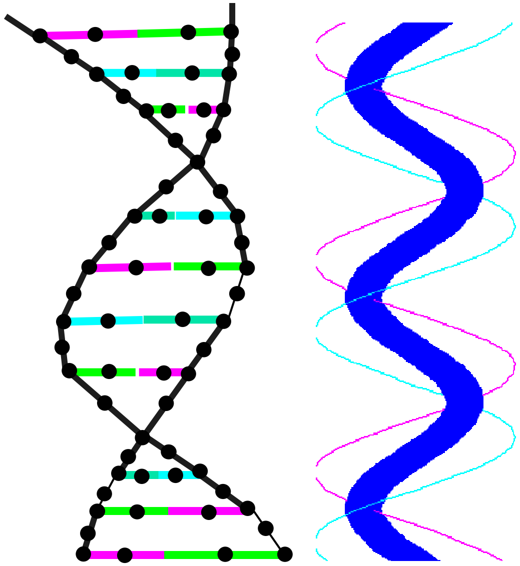

Under small deformation assumption

$$G = 8.75E + 08$$

$$E = 5.15E + 08$$

$$\nu = \frac{E - 2G}{2G} = -0.702$$

Experimental Poisson's ratio

$\nu = -0.7$ *Gerald S. Manning, Phys. Rev. A, 1986*

$0 > \nu > -0.4$ *C.G. Baumann, PNAS, 1997*

DNA Translocation through Nanopore

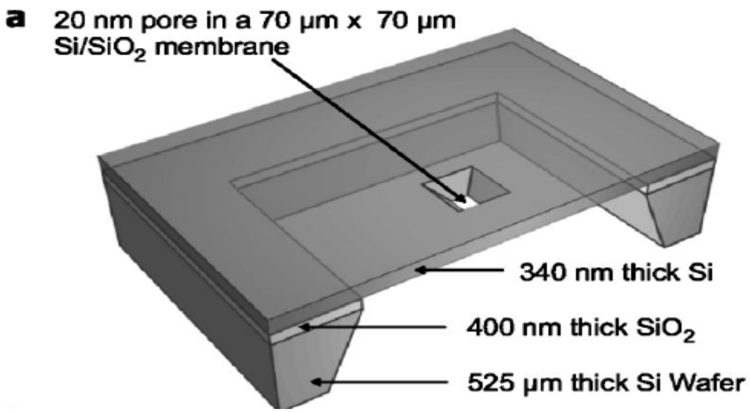

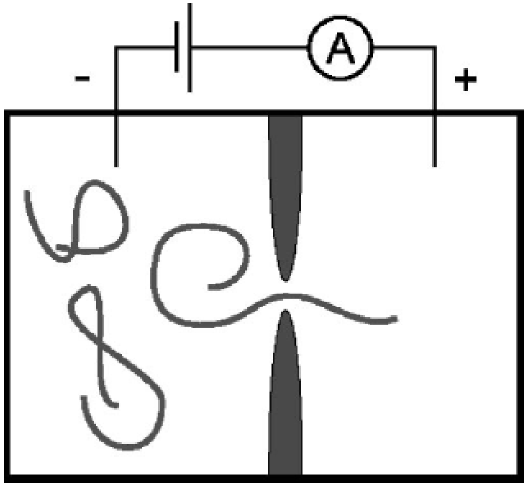

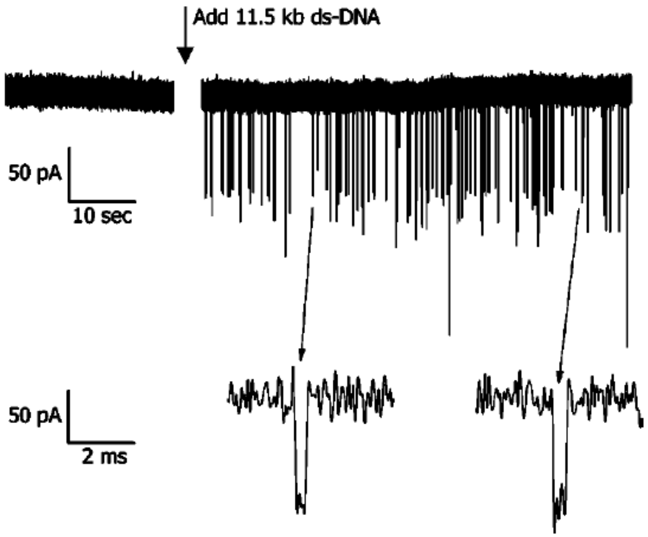

FIG. 4. Measured ionic current versus time. After addition of DNA to the *cis* side of the pore we clearly observe downward dips in the current. In the bottom panel, two individual events are shown at an increased time resolution.

A.J. Storm et al. PRE,2005

Numerical Simulation:
DNA Translocation through Nanopore

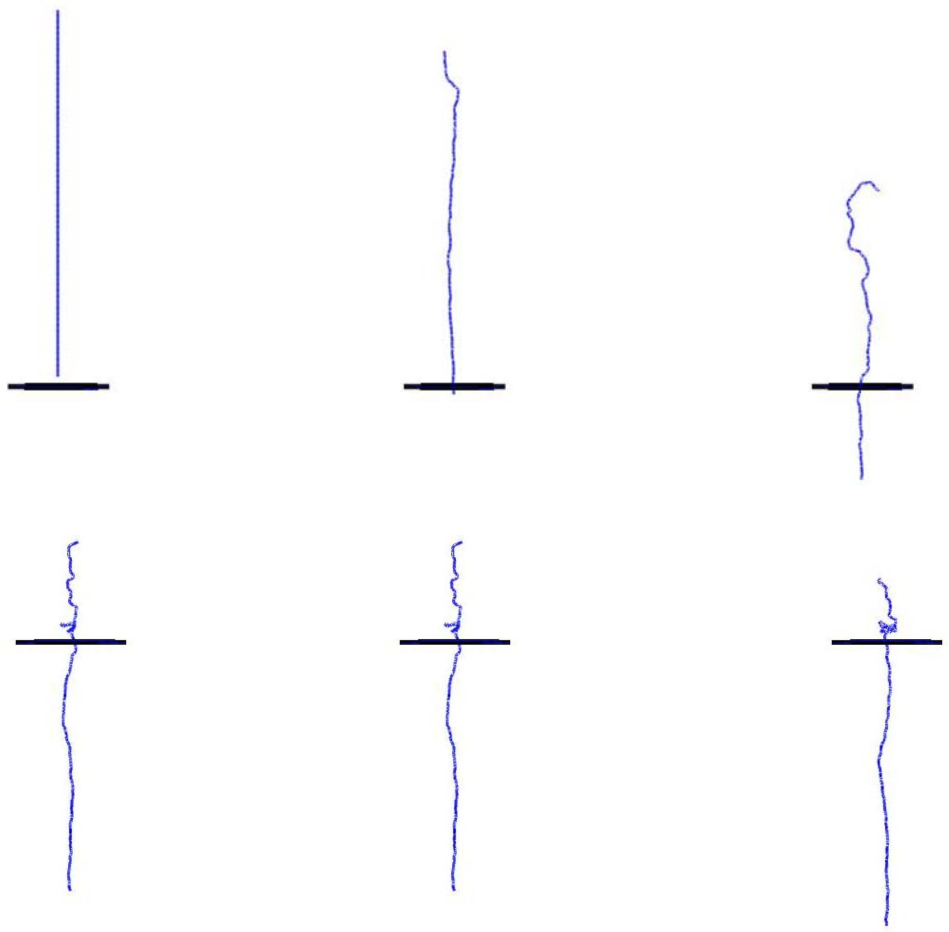

Animation

Numerical Simulation:
DNA Translocation through Nanopore

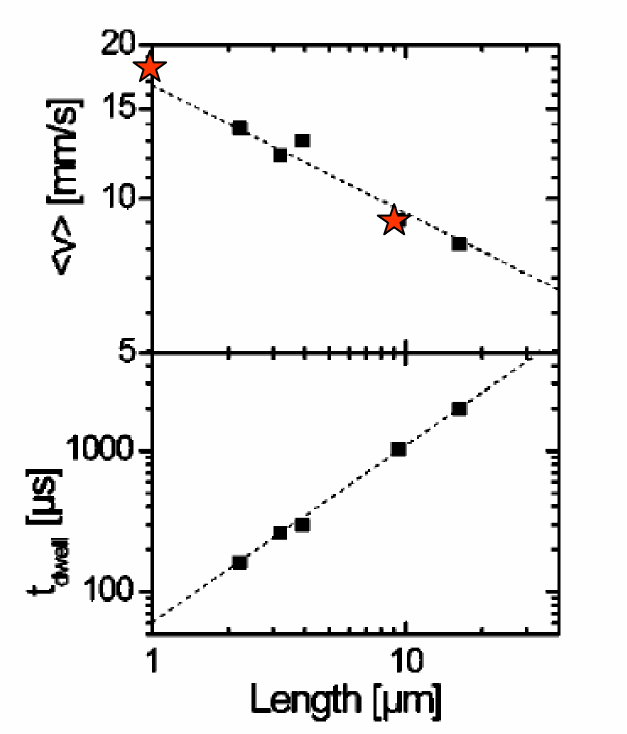

	DNA Length	Translocation Time	Averaged Velocity
Case 1	1088 nm	$58.5\mu s$	18.6mm/s
Case 2	10880 nm	$1250.5\mu s$	8.7mm/s

Hydrodynamics Model

$$\dot{R} = -\frac{B^{\frac{1}{D}}}{D}(L-x)^{\frac{1}{D}-1} v$$

$$f_{drag} = 6\pi\eta \frac{B^{\frac{2}{D}}}{D}(L-x)^{\frac{2}{D}-1} v = 6\pi\eta \frac{B^{\frac{2}{D}}}{D}(L-x)^{\frac{2}{D}-1} \frac{dx}{dt}$$

$$t = \frac{3\pi\eta B^{\frac{2}{D}}}{f_{drag}} L^{\frac{2}{D}} = \frac{C}{f_{drag}} L^{\frac{2}{D}} = \frac{C}{f_{drag}} L^{1.274}$$

$$t \sim L^{\alpha}$$

	Theoretical Estimation	Experimental Results(Storm)	Numerical Simulation
α	1.274	1.27 ± 0.03	1.33

UCLA

Quantum Mechanics

- **Governing equation**
  - Schrödinger equation (SE)

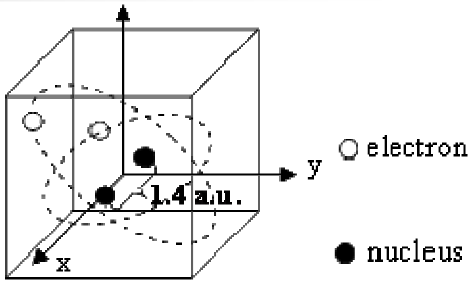

$$\hat{H}\psi\left(\mathbf{r}_1,\mathbf{r}_2,\ldots,\mathbf{r}_N\right)=E\psi\left(\mathbf{r}_1,\mathbf{r}_2,\ldots,\mathbf{r}_N\right)$$

  - Density functional theory (DFT)

$$\delta\left\{E\left(\rho(\mathbf{r})\right)-\mu\left[\int\rho(\mathbf{r})\,d\mathbf{r}-N\right]\right\}=0$$

- ***AB initio* Calculation (Molecular system)**
  - Hartree-Fock molecular orbital approximation (SE)

$$\left[-\frac{1}{2}\nabla_i^2+\hat{V}_i\right]\psi_i\left(\mathbf{r}_i\right)=\varepsilon_i\psi_i\left(\mathbf{r}_i\right)\qquad i=1,2,\ldots,N$$

  - Kohn and Sham Method (DFT)

$$\left[-\frac{1}{2}\nabla^2+\hat{V}_{KS}\left(\rho(\mathbf{r})\right)\right]\psi^{KS}\left(\rho(\mathbf{r})\right)=\varepsilon\psi^{KS}\left(\rho(\mathbf{r})\right)$$

AB initio

- **Basis set calculation**

$$\psi = \sum_{k=1}^{n} c_k \phi_k$$

- Gaussian-type orbital (GTO) with the radial form $e^{-\alpha r^2}$

$$g_s(\alpha, r) = \left(\frac{2\alpha}{\pi}\right)^{3/4} e^{-\alpha r^2}$$

$$g_x(\alpha, r) = \left(\frac{128\alpha^5}{\pi^3}\right)^{1/4} x e^{-\alpha r^2} \quad g_y(\alpha, r) = \left(\frac{128\alpha^5}{\pi^3}\right)^{1/4} y e^{-\alpha r^2} \quad g_z(\alpha, r) = \left(\frac{128\alpha^5}{\pi^3}\right)^{1/4} z e^{-\alpha r^2}$$

$$\vdots$$

- Slater-type orbital (STO) with the radial form $e^{-\alpha r}$
- Plane wave (PW)

Intrinsic Enrichment of Orbital Function

Intrinsic Enrichment

$$\phi_I(\mathbf{r}) = \varphi_I(\mathbf{r})\left[a_0(\mathbf{r}) + e^{-\xi r_I} a_1(\mathbf{r})\right], \quad r_I = \|\mathbf{r}_I\|$$

Reproducing Conditions:

$$\begin{cases} \sum_{I=1}^{N} \phi_I(\mathbf{r}) = 1 \\ \sum_{I=1}^{N} \phi_I(\mathbf{r}) e^{-\xi r_I} = e^{-\xi r} \end{cases} \Rightarrow \left\{ \sum_{I}^{N} \varphi_I(\mathbf{r}) \begin{bmatrix} 1 \\ e^{-\xi r_I} \end{bmatrix} \begin{bmatrix} 1 & e^{-\xi r_I} \end{bmatrix} \right\} \begin{bmatrix} a_0(\mathbf{r}) \\ a_1(\mathbf{r}) \end{bmatrix} = \begin{bmatrix} 1 \\ e^{-\xi r} \end{bmatrix}$$

$$\mathbf{A}(\mathbf{r})\mathbf{a}(\mathbf{r}) = \mathbf{b}(\mathbf{r})$$

$$\mathbf{A}(\mathbf{r}) = \sum_{I}^{N} \varphi_I(\mathbf{r})\mathbf{b}(\mathbf{r}_I)\mathbf{b}^T(\mathbf{r}_I) \quad \mathbf{b}^T(\mathbf{r}) = \begin{bmatrix} 1 & e^{-\xi r} \end{bmatrix} \quad \mathbf{a}^T(\mathbf{r}) = \begin{bmatrix} a_0(\mathbf{r}) & a_1(\mathbf{r}) \end{bmatrix}$$

$$\boxed{\phi_I(\mathbf{r}) = \mathbf{b}^T(\mathbf{r}_I)\mathbf{A}^{-1}(\mathbf{r})\mathbf{b}(\mathbf{r})\varphi_I(\mathbf{r})}$$

Chen, Hu. Puso, CMAME, 2007

Combined Intrinsic-Extrinsic Enrichment

$$\Psi^h(\mathbf{r}) = \sum_{I=1}^{N} \phi_I(\mathbf{r}) \left[\sum_{i=1}^{n} P_i(\mathbf{r} - \mathbf{r}_I) \alpha_I^i \right]$$

$$\phi_I(\mathbf{r}) = \mathbf{b}^T(\mathbf{r}_I) \mathbf{A}^{-1}(\mathbf{r}) \mathbf{b}(\mathbf{r}) \varphi_I(\mathbf{r})$$

$\mathbf{b}^T(\mathbf{r}) = \begin{bmatrix} 1 & e^{-\xi r} \end{bmatrix}$:Intrinsic basis function

$P_i(\mathbf{r} - \mathbf{r}_I)$: Extrinsic basis function

UCLA

Hydrogen Atom

$$\mathbf{h}_I^{in} = \left[1, e^{-\xi r} \right], \quad \mathbf{h}_I^{ex} = \left[1 \right]$$

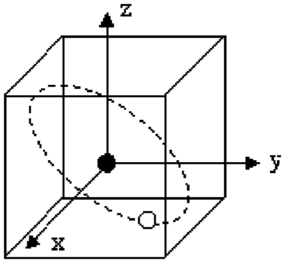

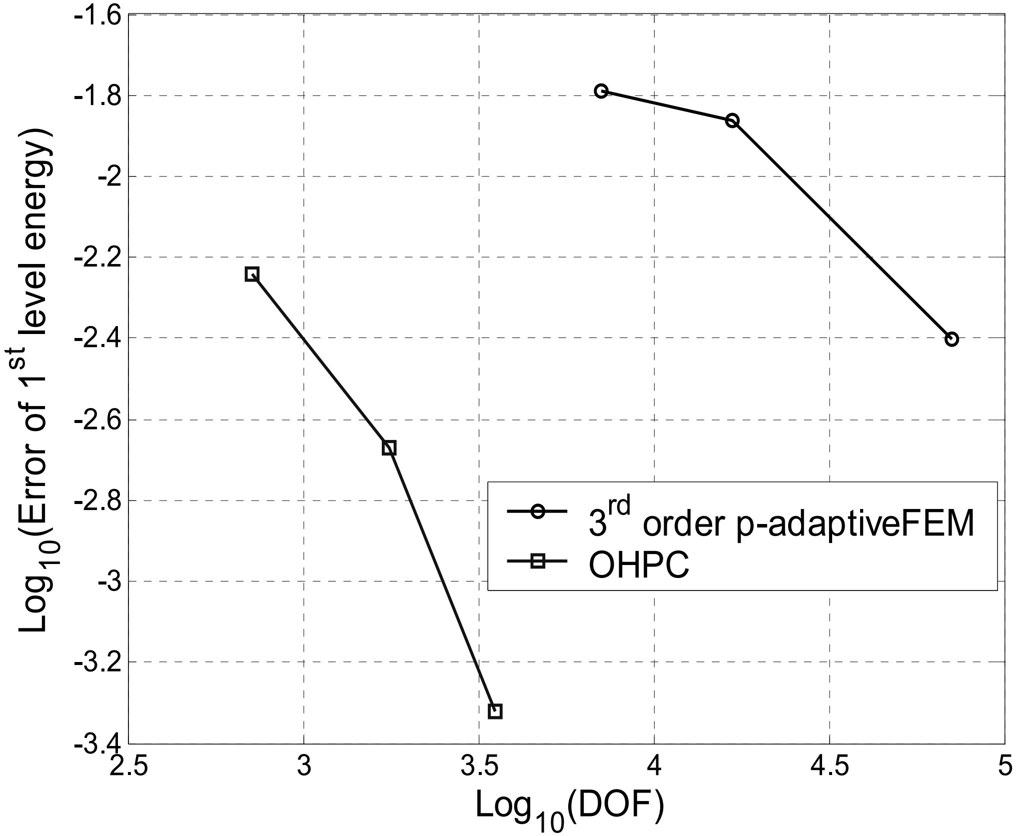

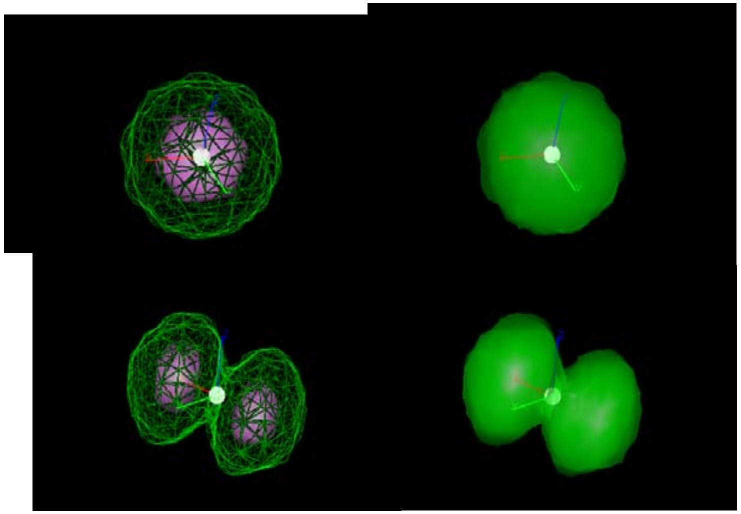

z

Hydrogen Molecule

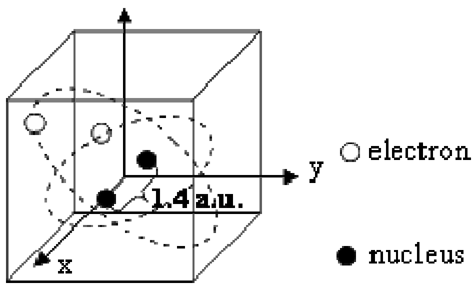

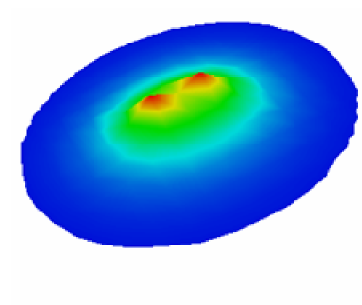

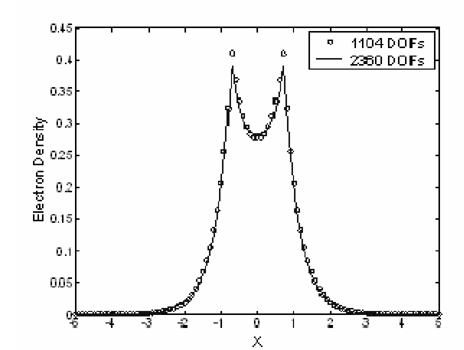

Electron density

Numerical Methods	No. of nodes	DOFs	Error of the first level energy
Gaussian-FEM	12,167	12,167	0.355%
OHPC $\mathbf{h}_I^{in} = \left[1, e^{-r_1}, e^{-r_2}\right]$ $\mathbf{h}_I^{ex} = \begin{cases} \left[1, \frac{x_1 - x_{1I}}{c_1}, \frac{x_2 - x_{2I}}{c_2}, \frac{x_3 - x_{3I}}{c_3}\right], & \lvert x_i \rvert \le 3 \text{ a.u.} \\ [1], & \lvert x_i \rvert > 3 \text{ a.u.} \end{cases}$	729	1,104	0.29%
	1,331	2,360	0.16%

Multiscale Modeling of Large-scale QDs

- **Hierarchical Structure of QDA Laser Generator**

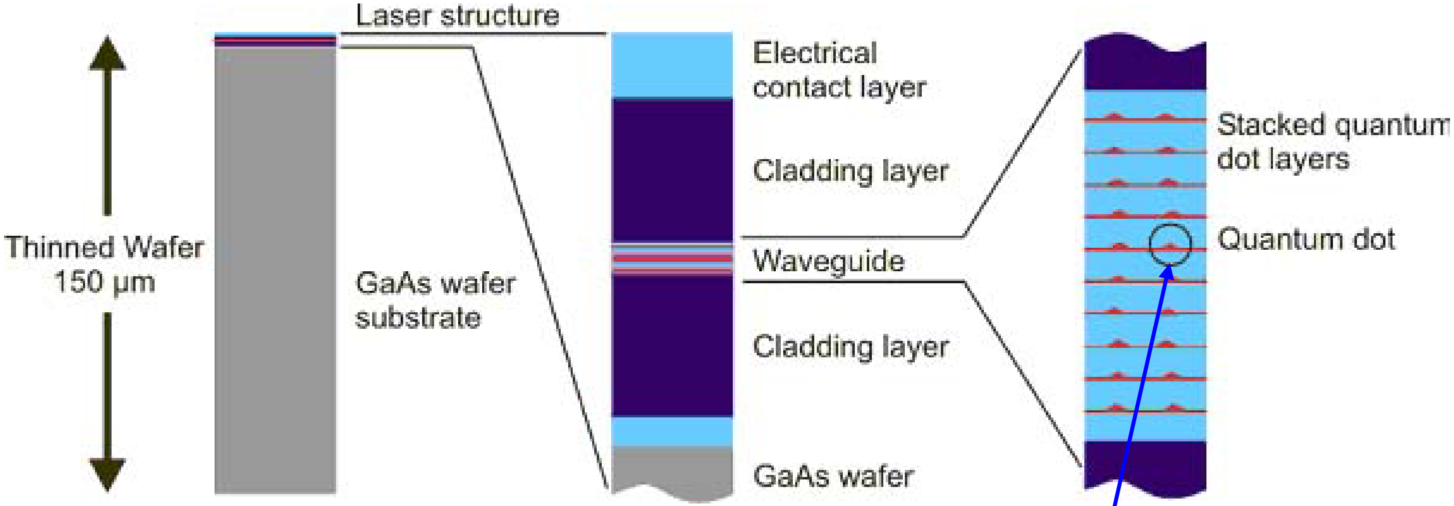

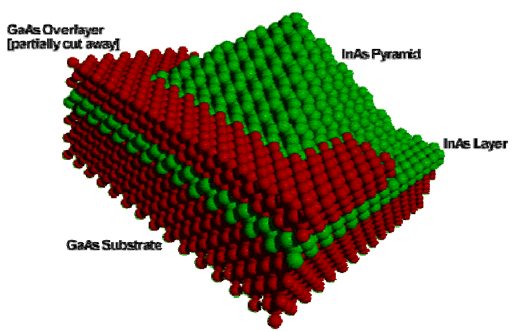

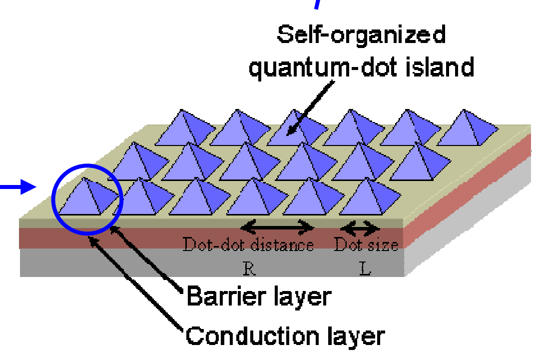

Multiscale Problem

Multiscale Coordinate System

$$y_i = \frac{x_i}{\lambda} \qquad i = 1, 2, 3$$

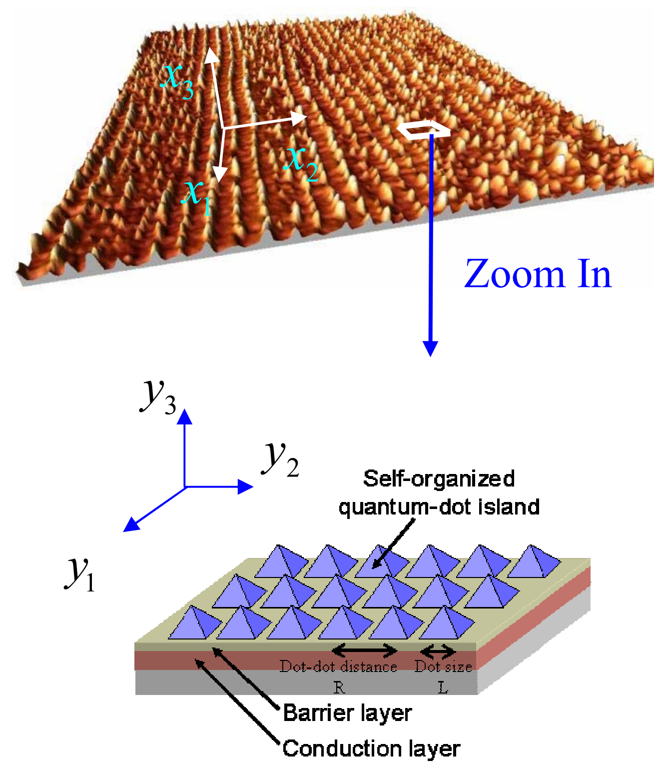

Total Eigen Value Problem

$$H_\lambda \Theta^\lambda = \varepsilon^\lambda \Theta^\lambda \quad \text{in} \quad \Omega$$

$$\Theta^\lambda = 0 \quad \text{on} \quad \Gamma$$

$$m^{*-} \frac{\partial \Theta^\lambda}{\partial \mathbf{n}^-} = m^{*+} \frac{\partial \Theta^\lambda}{\partial \mathbf{n}^+} \quad \text{on} \quad \Gamma^{\mathrm{I}}$$

where $$H_\lambda = -\frac{\hbar^2}{2} \nabla \cdot \left(\frac{1}{m^*(\boldsymbol{x}, \boldsymbol{y})} \nabla \right) + V(\boldsymbol{x}, \boldsymbol{y})$$

Homogeinzed Eigen Value Problem

$$H_0 \Theta^{[0]} = \varepsilon^{[0]} \Theta^{[0]} \quad \text{in} \quad \Omega$$

$$\Theta^{[0]} = 0 \quad \text{on} \quad \Gamma$$

$$m^{[0]*-} \frac{\partial \Theta^{[0]}}{\partial \mathbf{n}^-} = m^{[0]*+} \frac{\partial \Theta^{[0]}}{\partial \mathbf{n}^+} \quad \text{on} \quad \Gamma^{\mathrm{I},[0]}$$

$$\boxed{H_0 = -\frac{\hbar^2}{2} \nabla \cdot \left(\frac{1}{m^{[0]*}} \nabla \right) + V^{[0]}}$$

Auxiliary Problem

Strong Form

$$H_\lambda w^\lambda = \varepsilon^{[0]}\Theta^{[0]} \quad \text{in} \quad \Omega$$

$$w^\lambda = 0 \quad \text{on} \quad \Gamma$$

$$m^{*-}\frac{\partial w^\lambda}{\partial \mathbf{n}^-} = m^{*+}\frac{\partial w^\lambda}{\partial \mathbf{n}^+} \quad \text{on} \quad \Gamma^{\mathrm{I}}$$

$$As \quad \lambda \to 0, \quad w^{[0]} \to \Theta^{[0]}$$

Weak Form

$$a_\lambda\left(w^\lambda, v\right) = \varepsilon^{[0]}\left(\Theta^{[0]}, v\right)$$

$$w^\lambda = 0 \quad \text{on} \quad \Gamma$$

$$m^{*-}\frac{\partial w^\lambda}{\partial \boldsymbol{n}^-} = m^{*+}\frac{\partial w^\lambda}{\partial \boldsymbol{n}^+} \quad \text{on} \quad \Gamma^{\mathrm{I}}$$

Scale Coupling

Bridging Between Coarse Scale and Fine Scale

$$w^{[1]}(\boldsymbol{x},\boldsymbol{y}) = \alpha_j(y_j)\frac{\partial\Theta^{[0]}(\boldsymbol{x})}{\partial x_j} + \beta(\boldsymbol{y})\Theta^{[0]}(\boldsymbol{x})$$

$$H_\lambda w^\lambda = \varepsilon^{[0]}\Theta^{[0]} \longrightarrow \boxed{\begin{array}{ll} O\left(\lambda^{-1}\dfrac{\partial\Theta^{[0]}(\boldsymbol{x})}{\partial x_j}\right): & H_{-2}\alpha_j(y_j) = -L_{-2}y_j \\ O\left(\lambda^{-1}\Theta^{[0]}(\boldsymbol{x})\right): & H_{-2}\beta(\boldsymbol{y}) = -\tilde{V} \end{array}}$$

$$m^{*-}\frac{\partial w^\lambda}{\partial \boldsymbol{n}^-} = m^{*+}\frac{\partial w^\lambda}{\partial \boldsymbol{n}^+} \xrightarrow{\text{on } \Gamma^{\mathrm{I}}} \boxed{\begin{array}{l} m^{*-}\dfrac{\partial\alpha_j}{\partial \boldsymbol{n}^-} = m^{*+}\dfrac{\partial\alpha_j}{\partial \boldsymbol{n}^+} \\ m^{*-}\dfrac{\partial\beta}{\partial \boldsymbol{n}^-} = m^{*+}\dfrac{\partial\beta}{\partial \boldsymbol{n}^+} \end{array}}$$

Homogenized Material Constants

Homogenized Effective Mass and Confinement Potential

$$a_\lambda\left(w^\lambda, v\right)=\varepsilon^{[0]}\left(\Theta^{[0]}, v\right)\rightarrow$$

$$\int_\Omega\int_{\Omega_y}\left(\frac{\partial v^{[0]}}{\partial x_i}+\frac{\partial\alpha_k}{\partial y_i}\frac{\partial v^{[0]}}{\partial x_k}+\frac{\partial\beta}{\partial y_i}v^{[0]}\right)\frac{1}{m^*\left(\boldsymbol{x},\boldsymbol{y}\right)}\delta_{ij}\left(\frac{\partial\Theta^{[0]}}{\partial x_j}+\frac{\partial\alpha_l}{\partial y_j}\frac{\partial\Theta^{[0]}}{\partial x_l}+\frac{\partial\beta}{\partial y_j}\Theta^{[0]}\right)d\boldsymbol{y}d\Omega$$

$$+\int_\Omega\int_{\Omega_y}2\beta\tilde{V}\left(\boldsymbol{x},\boldsymbol{y}\right)v^{[0]}\Theta^{[0]}d\boldsymbol{y}d\Omega=A_{\Omega_y}\varepsilon^{[0]}\int_\Omega\left(\Theta^{[0]}v^{[0]}\right)d\Omega$$

$$H_{-2}\alpha_j\left(y_j\right)=-L_{-2}y_j$$

$$H_{-2}\beta\left(\boldsymbol{y}\right)=-\tilde{V}^\lambda$$

$$\rightarrow$$

$$\int_{\Omega_y}\left[\frac{1}{m^*\left(\boldsymbol{x},\boldsymbol{y}\right)}\frac{\partial\left(\alpha_i+y_i\right)}{\partial y_j}\frac{\partial\beta}{\partial y_j}\right]d\boldsymbol{y}=0$$

$$\int_{\Omega_y}\left[\frac{1}{m^*\left(\boldsymbol{x},\boldsymbol{y}\right)}\frac{\partial\beta}{\partial y_i}\frac{\partial\beta}{\partial y_i}+\beta\tilde{V}\left(\boldsymbol{x},\boldsymbol{y}\right)\right]d\boldsymbol{y}=0$$

$$\boxed{\int_\Omega\frac{\partial v^{[0]}}{\partial x_i}\frac{1}{m_{ii}^{[0]}\left(\boldsymbol{x}\right)}\frac{\partial\Theta^{[0]}}{\partial x_j}d\Omega+\int_\Omega V^{[0]}\left(\boldsymbol{x}\right)v^{[0]}\Theta^{[0]}d\Omega=A_{\Omega_y}\varepsilon^{[0]}\int_\Omega\left(\Theta^{[0]}v^{[0]}\right)d\Omega}$$

$$\frac{1}{m_{ii}^{[0]}\left(\boldsymbol{x}\right)}=\frac{1}{A_{\Omega_y}}\int_{\Omega_y}\left[\frac{\partial\left(\alpha_i+y_i\right)}{\partial y_i}\right]^2\frac{1}{m^*\left(\boldsymbol{x},\boldsymbol{y}\right)}d\boldsymbol{y},\quad V^{[0]}\left(\boldsymbol{x}\right)=\frac{1}{A_{\Omega_y}}\int_{\Omega_y}\beta\tilde{V}\left(\boldsymbol{x},\boldsymbol{y}\right)d\boldsymbol{y}$$

Numerical Examples

- **A Series of QDA in One Dimension**
  - Each QDA: randomly oscillating effective mass and confinement potential
  - Full model as reference

    Quadratic basis function

    553 nodes
  - Multiscale model

    Linear basis function

    Coarse scale domain:

    31 nodes

    Three fine scale unit cells

    93 nodes in each cell

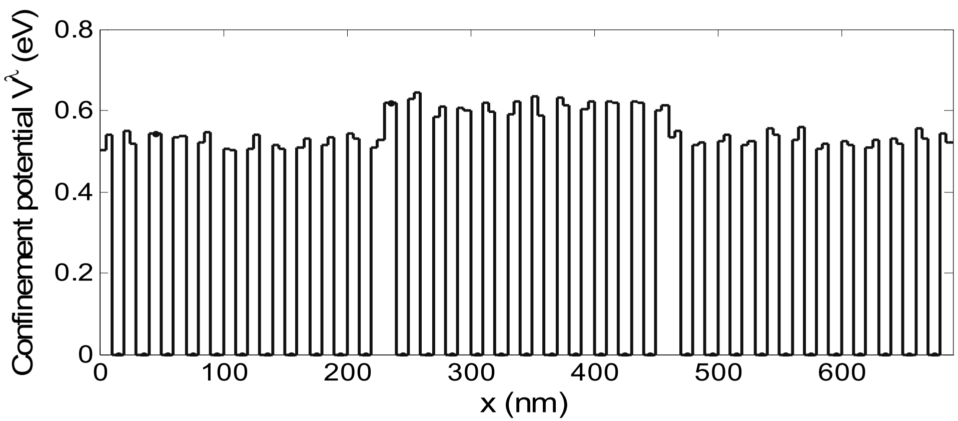

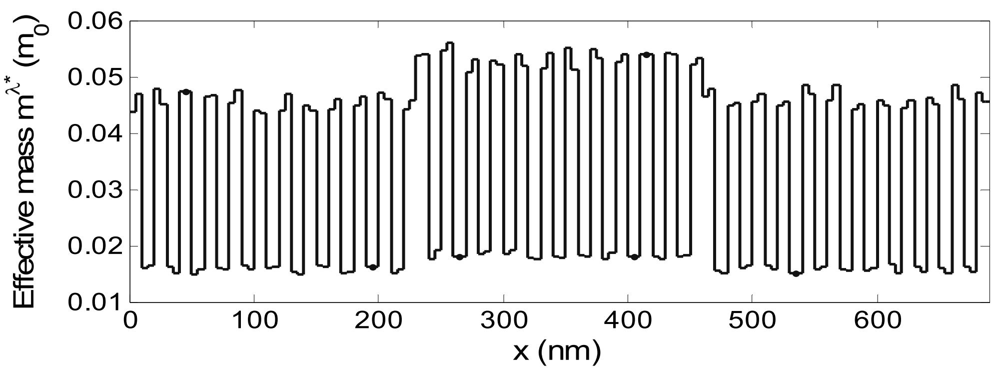

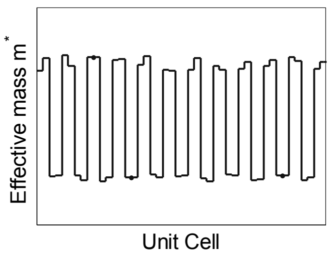

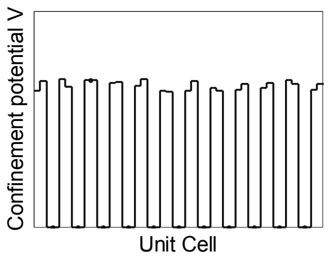

UCLA

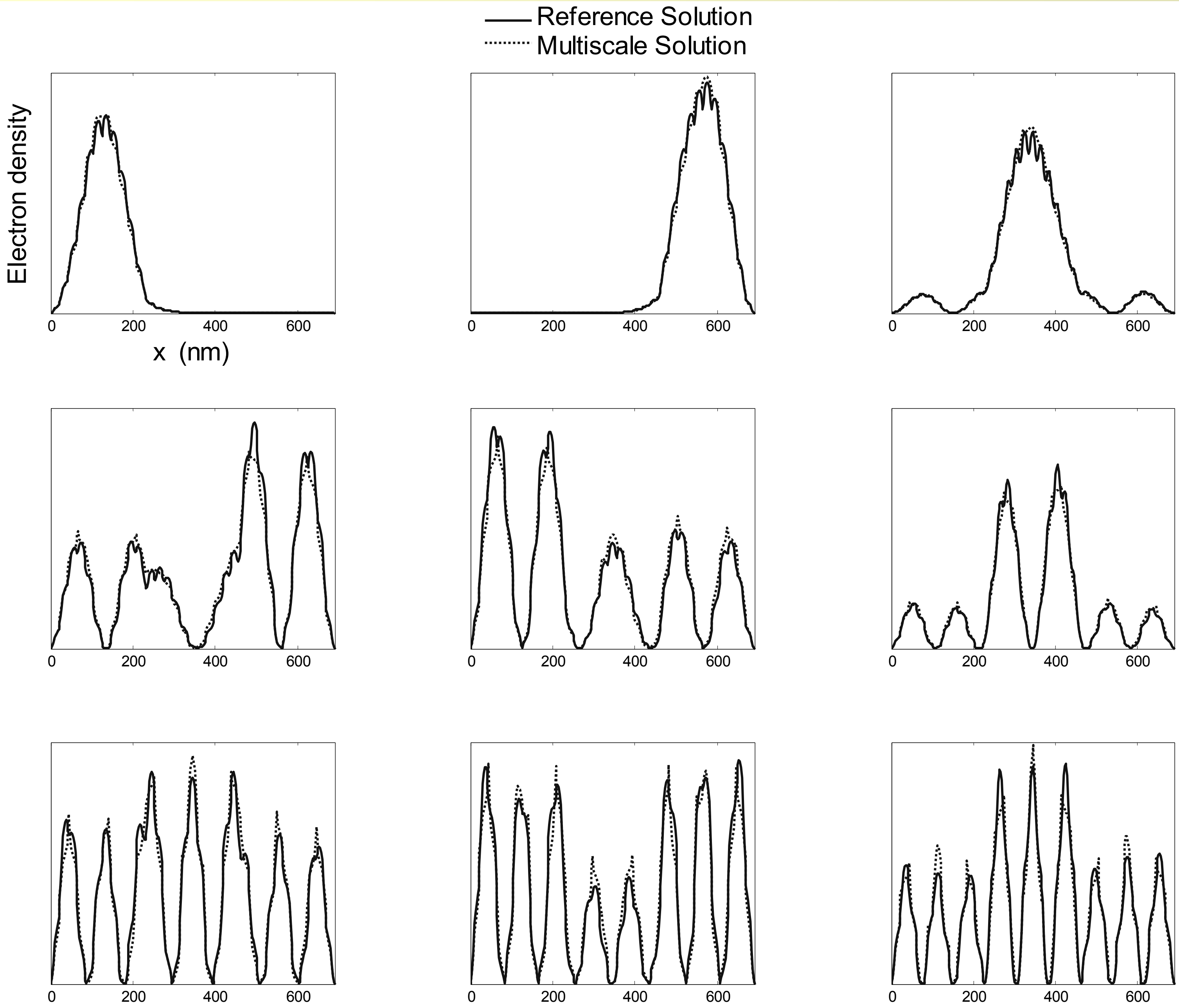
Reference Solution
Multiscale Solution
Electron density
x (nm)
0
200
400
600

Radial Basis Function Approximation

- **Radial Basis Functions:**
  - Multiquadrics (MQ): $g_I(\mathbf{x}) = \left(r_I^2 + c^2\right)^{n-\frac{3}{2}}$
  - Gaussian: $g_I(\mathbf{x}) = \exp\left(-r_I^2/c^2\right)$
  - Thin plate splines $g_I(\mathbf{x}) = r_I^{2n}\ln r_I, \quad r_I^{2n-1}$
  - Logarithmic $g_I(\mathbf{x}) = r_I^n \ln r_I$

- **RBF Approximation:**
  - A set of N_s source points: $\mathbf{S} = [\mathbf{x}_1, \mathbf{x}_2, \cdots \mathbf{x}_{N_s}] \subseteq \Omega \cup \partial\Omega$
  - The approximation $v(\mathbf{x})$ for a smooth function $u(\mathbf{x})$:

$$v(\mathbf{x}) = \sum_{I=1}^{N_s} g_I(\mathbf{x}) a_I = \mathbf{\Phi}^T \mathbf{a}$$

- **Exponential convergence rate** (Madych, Nelson, 1992)

$$\left|u(\mathbf{x}) - v(\mathbf{x})\right| \approx O\left(\eta^{c/h}\right)$$

UCLA

Direct Collocation Method (DCM)

Strong Form

$$\mathbf{Lu} = \mathbf{f} \quad in \quad \Omega$$

$$\mathbf{B}^h \mathbf{u} = \mathbf{h} \quad on \quad \partial\Omega^h$$

$$\mathbf{B}^g \mathbf{u} = \mathbf{g} \quad on \quad \partial\Omega^g$$

A Set of Collocation Points

$$\mathbf{P} = [\mathbf{p}_1, \mathbf{p}_2, \cdots \mathbf{p}_{N_p}] \subseteq \Omega$$

$$\mathbf{Q} = [\mathbf{q}_1, \mathbf{q}_2, \cdots \mathbf{q}_{N_q}] \subseteq \partial\Omega^h$$

$$\mathbf{R} = [\mathbf{r}_1, \mathbf{r}_2, \cdots \mathbf{r}_{N_r}] \subseteq \partial\Omega^g$$

Residuals are forced to be zero at collocation points: $\boxed{\mathbf{A}\tilde{\mathbf{a}} = \mathbf{b}}$

$$\mathbf{A} = \begin{pmatrix} \mathbf{A}^1 \\ \mathbf{A}^2 \\ \mathbf{A}^3 \end{pmatrix}: \quad \mathbf{A}^1 = \begin{pmatrix} \mathbf{L}\left(\tilde{\boldsymbol{\Phi}}^{\mathrm{T}}(\mathbf{p}_1)\right) \\ \mathbf{L}\left(\tilde{\boldsymbol{\Phi}}^{\mathrm{T}}(\mathbf{p}_2)\right) \\ \vdots \\ \mathbf{L}\left(\tilde{\boldsymbol{\Phi}}^{\mathrm{T}}(\mathbf{p}_{N_p})\right) \end{pmatrix}, \quad \mathbf{A}^2 = \begin{pmatrix} \mathbf{B}^h\left(\tilde{\boldsymbol{\Phi}}^{\mathrm{T}}(\mathbf{q}_1)\right) \\ \mathbf{B}^h\left(\tilde{\boldsymbol{\Phi}}^{\mathrm{T}}(\mathbf{q}_2)\right) \\ \vdots \\ \mathbf{B}^h\left(\tilde{\boldsymbol{\Phi}}^{\mathrm{T}}(\mathbf{q}_{N_q})\right) \end{pmatrix}, \quad \mathbf{A}^3 = \begin{pmatrix} \mathbf{B}^g\left(\tilde{\boldsymbol{\Phi}}^{\mathrm{T}}(\mathbf{r}_1)\right) \\ \mathbf{B}^g\left(\tilde{\boldsymbol{\Phi}}^{\mathrm{T}}(\mathbf{r}_2)\right) \\ \vdots \\ \mathbf{B}^g\left(\tilde{\boldsymbol{\Phi}}^{\mathrm{T}}(\mathbf{r}_{N_r})\right) \end{pmatrix}$$

$$\mathbf{b} = \begin{pmatrix} \mathbf{b}^1 \\ \mathbf{b}^2 \\ \mathbf{b}^3 \end{pmatrix}: \quad \mathbf{b}^1 = \begin{pmatrix} \mathbf{f}(\mathbf{p}_1) \\ \mathbf{f}(\mathbf{p}_2) \\ \vdots \\ \mathbf{f}(\mathbf{p}_{N_p}) \end{pmatrix}, \quad \mathbf{b}^2 = \begin{pmatrix} \mathbf{h}(\mathbf{q}_1) \\ \mathbf{h}(\mathbf{q}_2) \\ \vdots \\ \mathbf{h}(\mathbf{q}_{N_q}) \end{pmatrix}, \quad \mathbf{b}^3 = \begin{pmatrix} \mathbf{g}(\mathbf{r}_1) \\ \mathbf{g}(\mathbf{r}_2) \\ \vdots \\ \mathbf{g}(\mathbf{r}_{N_r}) \end{pmatrix}$$

Radial Basis Function Approximation

- **Disadvantages**
  - Unbalanced error between domain and boundary

  * Propose weighted RBF collocation method

  - Global approximation
  - ILL-Conditioning
  - Difficult to perform local refinement and special function enrichment

  * Propose local radial basis function approximation

  - No reproducibility of constant and linear functions in finite domain with finite number of source points

  * Introduce reproducing kernel as localized function for RBF, which po ssesses polynomial reproducibility

UCLA

Direct Collocation Method (DCM)

- **Over-determinant Problem**

$$N_p + N_q + N_r > N_s$$

$$\Pi = \frac{1}{2}(\mathbf{Aa}-\mathbf{b})^T(\mathbf{Aa}-\mathbf{b}) \longrightarrow \frac{\partial \Pi}{\partial \mathbf{a}} = \mathbf{A}^T(\mathbf{Aa}-\mathbf{b}) = \mathbf{0} \longrightarrow \boxed{\mathbf{A}^T\mathbf{Aa} = \mathbf{A}^T\mathbf{b}}$$

- **Least-Squares Functional**

$$\min E(v) = \frac{1}{2}\int_{\Omega}(\mathbf{L}v-\mathbf{f})^T(\mathbf{L}v-\mathbf{f})d\Omega + \frac{1}{2}\int_{\partial\Omega^h}(\mathbf{B}^h v-\mathbf{h})^T(\mathbf{B}^h v-\mathbf{h})d\Gamma + \frac{1}{2}\int_{\partial\Omega^g}(\mathbf{B}^g v-\mathbf{g})^T(\mathbf{B}^g v-\mathbf{g})d\Gamma$$

- **Large solution error near boundaries!**
  - The residuals of domain and boundary terms are minimized with the same weight
  - Relatively small number of boundary collocation points results in large error on the boundaries

Weighted Direct Collocation Method (W-DCM)

$$E(v)=\frac{1}{2}\int_{\Omega}(\mathbf{L}v-\mathbf{f})^T(\mathbf{L}v-\mathbf{f})d\Omega+\frac{\alpha_h}{2}\int_{\partial\Omega^h}(\mathbf{B}^h v-\mathbf{h})^T(\mathbf{B}^h v-\mathbf{h})d\Gamma+\frac{\alpha_g}{2}\int_{\partial\Omega^g}(\mathbf{B}^g v-\mathbf{g})^T(\mathbf{B}^g v-\mathbf{g})d\Gamma$$

- **Poisson Problem**
  - Define $\|v\|_B=\left(\|\mathbf{L}v\|_{0,\Omega}^2+\|v\|_{1,\Omega}^2+\alpha^h\|\mathbf{B}^h v\|_{0,\partial\Omega^h}^2+\alpha^g\|\mathbf{B}^g v\|_{0,\partial\Omega^g}^2\right)^{\frac{1}{2}}$
  - Error estimation:

    $$\|u-u_{N_s}\|_B\le\left(\bar{C}_1 N_s+\bar{C}_2\sqrt{\alpha^h}N_s+\bar{C}_3\sqrt{\alpha^g}\right)\|u-v\|_{1,\Omega}$$

  - For Balance of Error : $\boxed{\sqrt{\alpha^h}\approx O(1),\quad \sqrt{\alpha^g}\approx O(N_s)}$

- **Linear Elasticity**
  - Error estimation: $\kappa=\max\{\lambda,\mu\}$

    $$\|\mathbf{u}-\mathbf{u}_{N_s}\|_B\le\left(C_1'\kappa N_s+C_2'\kappa N_s\sqrt{\alpha^h}+C_3'\sqrt{\alpha^g}\right)\|u_1-v_1\|_{1,\Omega}$$
    $$+\left(C_3'\kappa N_s+C_4'\kappa N_s\sqrt{\alpha^h}+C_5'\sqrt{\alpha^g}\right)\|u_2-v_2\|_{1,\Omega}$$

  - For Balance of Error : $\boxed{\sqrt{\alpha^h}\approx O(1),\quad \sqrt{\alpha^g}\approx O(\kappa N_s)}$

UCLA

Hu, Chen, Hu, IJNME, 2007

Numerical Examples

- **Poisson Problem**

$$\Delta u(x,y) = (x^2+y^2)e^{xy} \qquad \Omega = (0,1)\times(0,1)$$

$$u(x,y) = e^{xy} \qquad \partial\Omega$$

- MQ-RBF

$$g_I(\mathbf{x}) = \frac{1}{\sqrt{r_I^2 + c^2}}$$

where $c = 1.6$

- Source points:

$6\times 6, 8\times 8, 10\times 10$

- Collocation points: 13×13

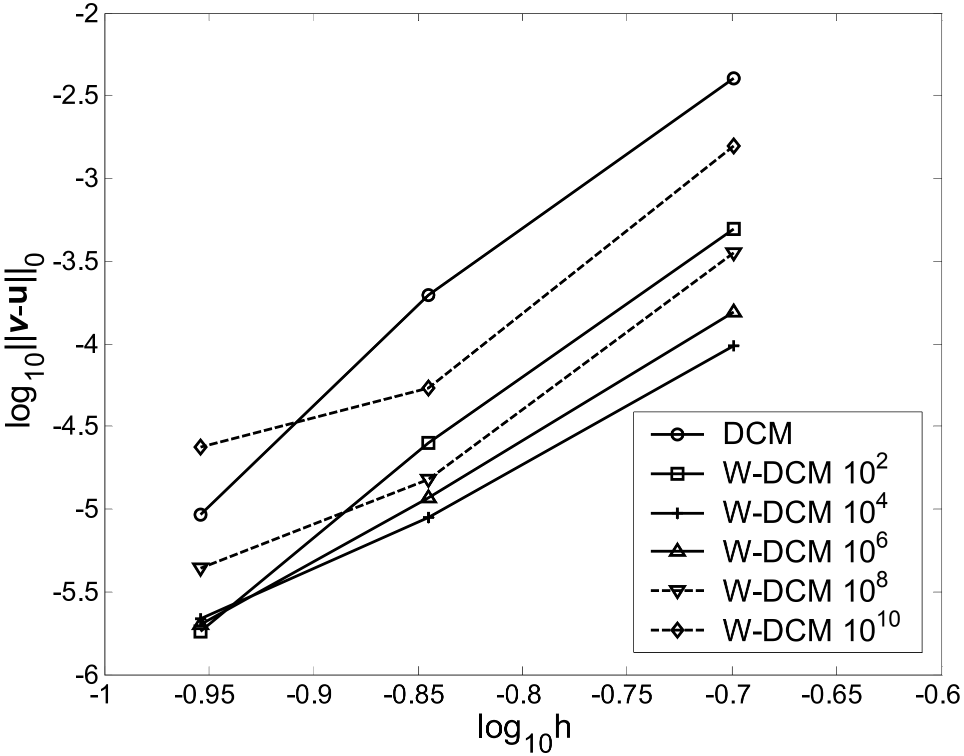

Numerical Examples

- **Poisson Problem**

Solution error:

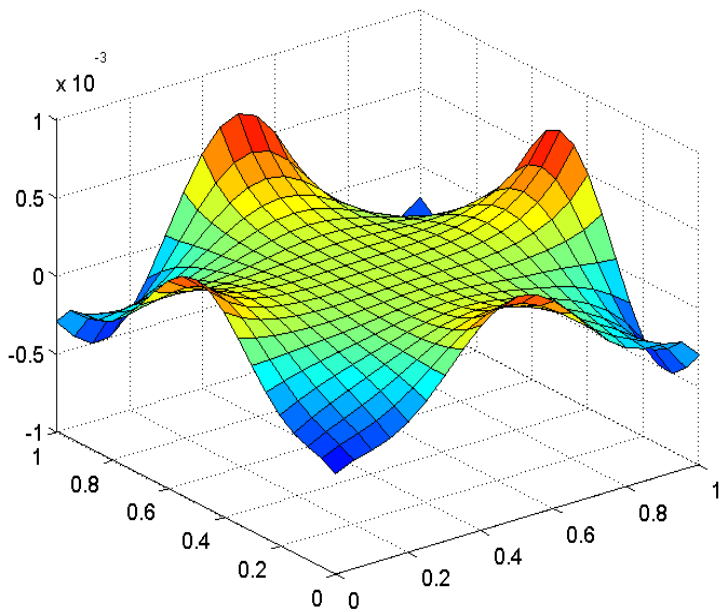

DCM

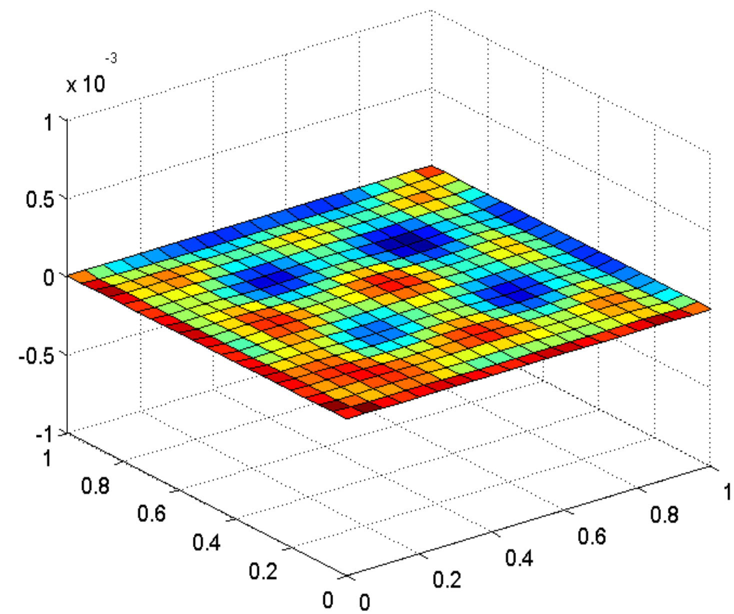

W-DCM

Local Radial Basis Function (L-RBF)

- **Local RBF with Monomial Reproducibility**

$$u^h(\mathbf{x}) = \sum_{I=1}^{N_s} \left[\phi_I(\mathbf{x}) \left(a_I^0 + g_I(\mathbf{x}) a_I^1 \right) \right] = \tilde{\mathbf{\Phi}}^T \tilde{\mathbf{a}}$$

where $\phi_I(\mathbf{x})$: **RK shape functions**

$g_I(\mathbf{x})$: **RBF**

- Locality is controlled by $\phi_I(\mathbf{x})$
- Partition of Unity and monomial reproducibility: $\sum_{I=1}^{N_s} \left[\phi_I(\mathbf{x}) a_I^0 \right]$
- Exponential convergence: $\sum_{I=1}^{N_s} \left[\phi_I(\mathbf{x}) g_I(\mathbf{x}) a_I^1 \right]$

W-DCM with L-RBF Approximation

- **Error Bound**

$$\left\| u - u^h \right\|_{l,\Omega} \le \left\{ C_1 \chi \eta_l^{c/h} + C_2 \chi a^{-l} \eta_0^{c/h} \right\} \left\| u \right\|_g , \quad 0 < \eta_l , \eta_0 < 1$$

where C_1, C_2 : genetic constants

χ : maximal number of covers for any point position

p : the highest order of polynomial reproduced by RK kernel

$a = (p+1)h$

- The errors decay *exponentially*

- **Condition Number**

$$cond(\tilde{A}) \le C_1 \chi^{1/2} a^{-d} p^{2d} + C_2 \chi^{1/2} a^{-3d/2} \left(p^{2d} + \mu^d \right)$$

where d : space dimension; μ : number of source points covered by RK support

$$1 < p < \chi, \mu \ll N_s$$

UCLA

W-DCM with L-RBF Approximation

- **Comparison of Condition Numbers in 2D Problem**

  - RBF: $cond. \approx O\left(h^{-8}\right)$
  - RK: $cond. \approx O\left(\chi^{1/2} a^{-2} p^{4}\right) = O\left(h^{-2}\right)$
  - Wendland function: $cond. \approx O\left(h^{-6-2k}\right)$ $k = 0, 1, 2, 3$
  - L-RBF: $cond. \approx O\left(\chi^{1/2} a^{-3} \mu^{2}\right) \approx O\left(h^{-3}\right)$

Numerical Examples

- **2-D Poisson Problem** $\Delta u(x,y) = (x^2+y^2)e^{xy} \quad \Omega = (0,1)\times(0,1)$

$$u(x,y) = e^{xy} \qquad \partial\Omega$$

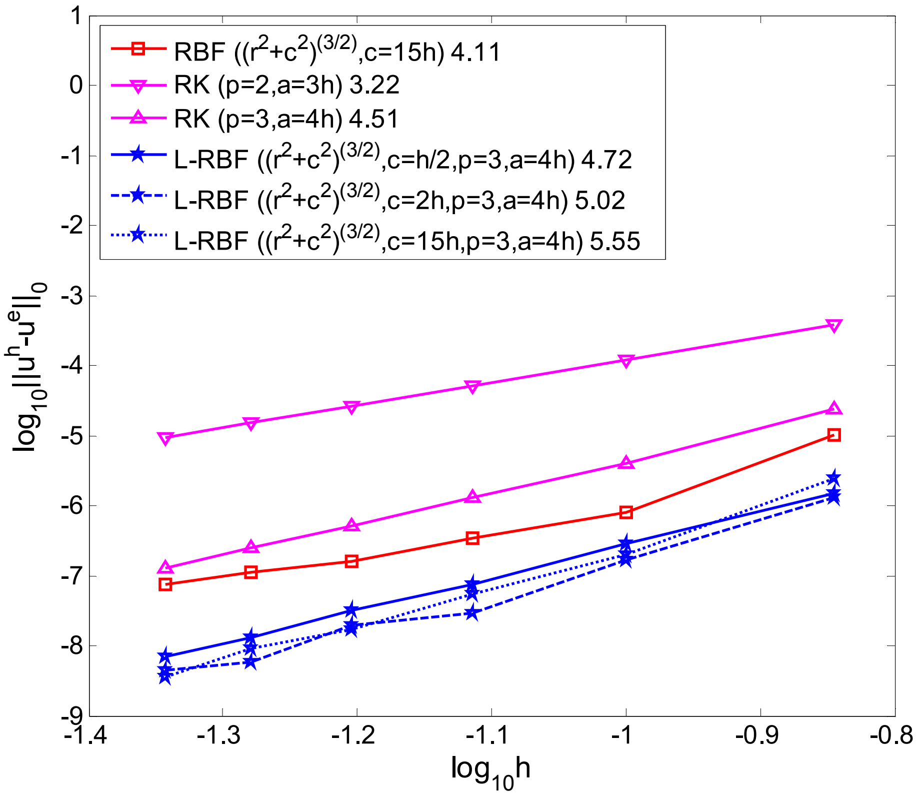

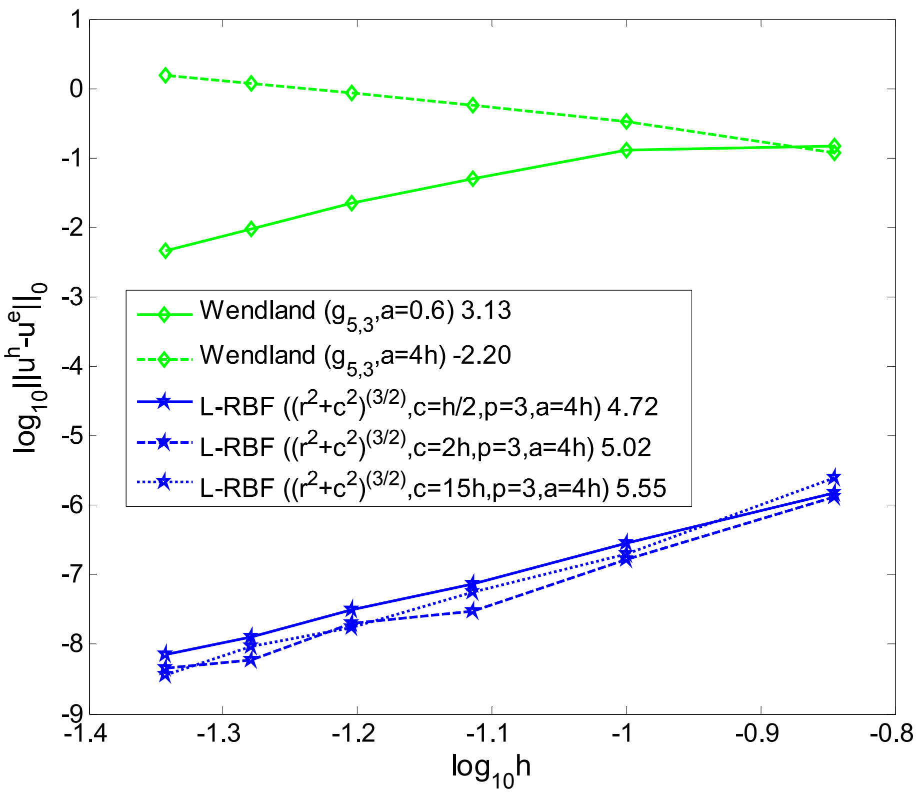

UCLA

Numerical Examples

- **2-D Poisson Problem**

$$\Delta u(x,y) = (x^2 + y^2) e^{xy} \qquad \Omega = (0,1)\times(0,1)$$

$$u(x,y) = e^{xy} \qquad \partial\Omega$$

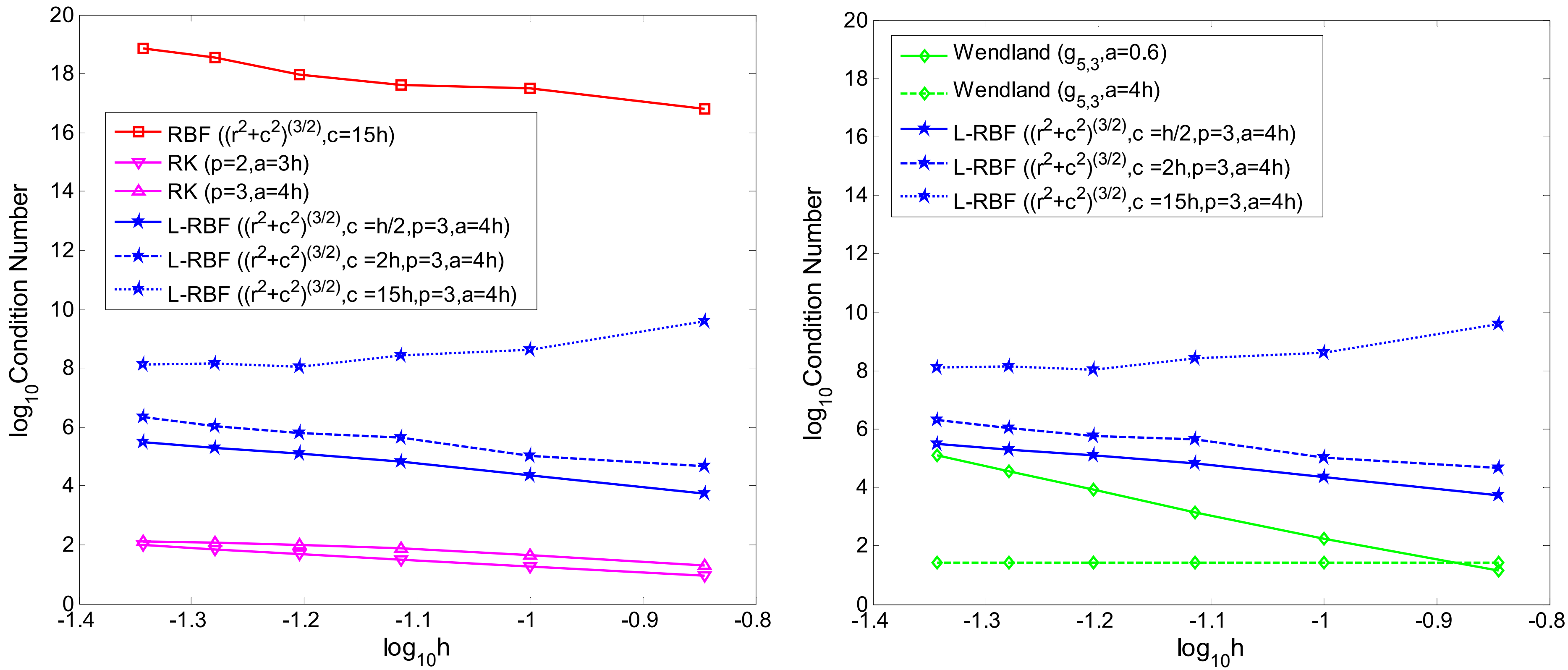

UCLA

Spherical Quantum Dot

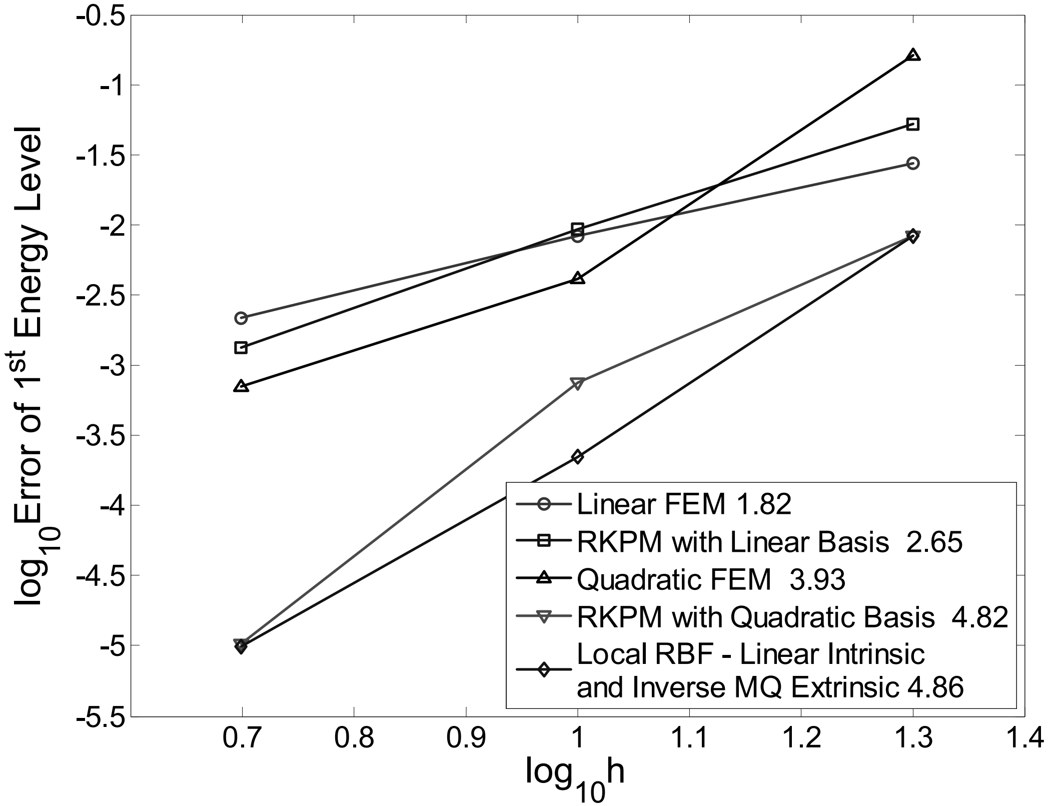

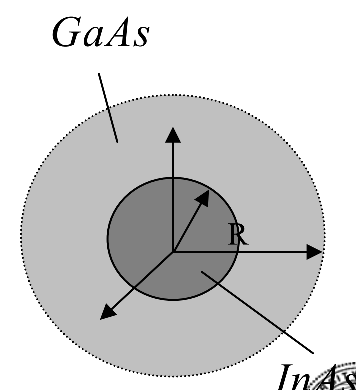

Interface Enrichment Function

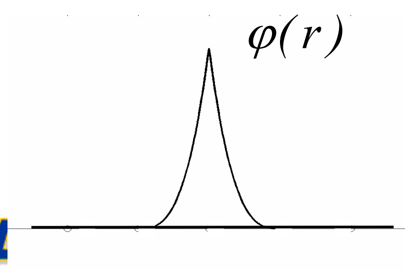

$\times$

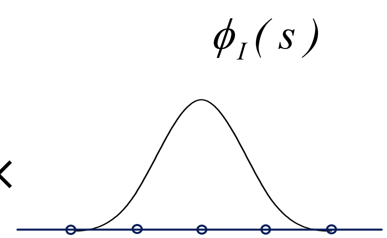

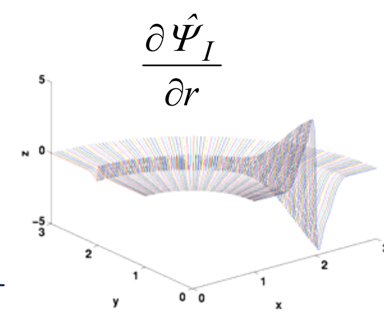

Quantum Dots Array

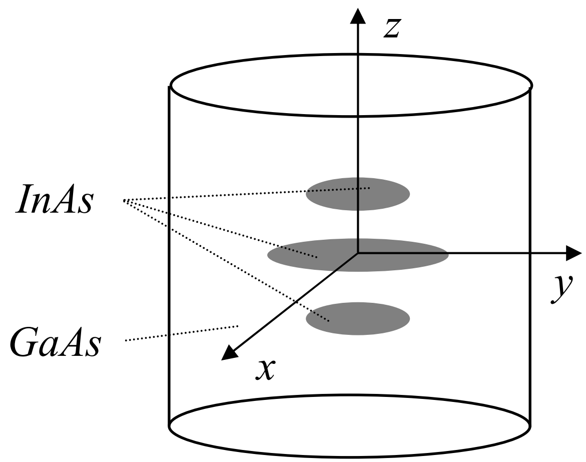

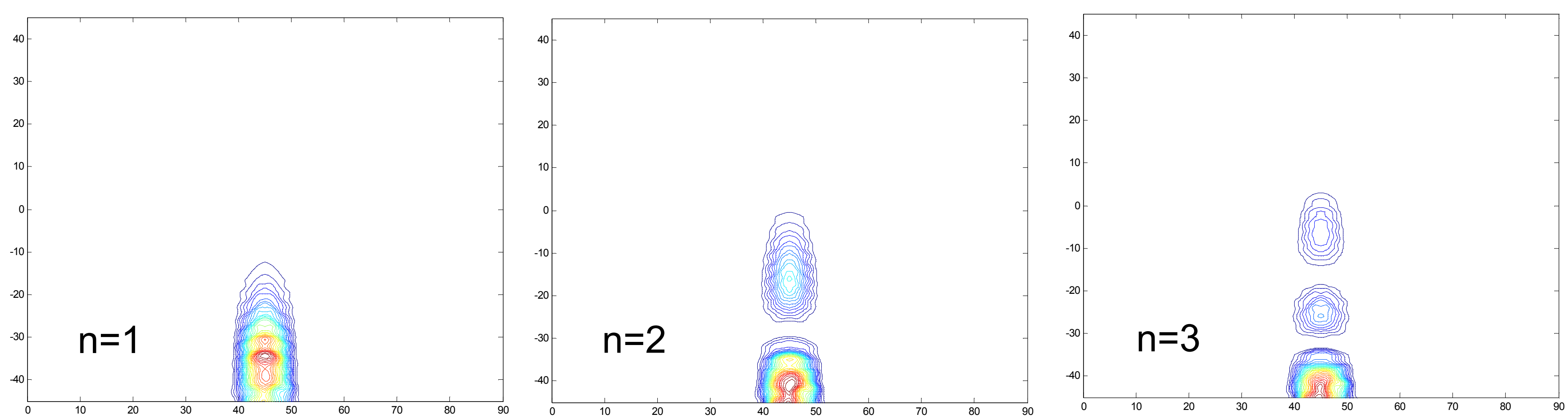

Conclusions

- **Galerkin Weak Form**
  - Algebraic Convergence
  - Easy Coupling with FEM, Adaptive Refinement
  - Domain Integration Plays a Key Role
    - Accuracy & Convergence
    - Spatial Stability
    - Temporal Stability
- **Strong Collocation Form**
  - Exponential Convergence: RBF Global Approximation
    - ILL-conditioning
    - Full discrete system
  - Enhanced Approaches
    - Weighted Collocation
    - Localized RBF